Chemical Geology 558 (2020) 119949

Contents lists available at ScienceDirect

Chemical Geology

journal homepage: www.elsevier.com/locate/chemgeo

Linking the karst record to atmospheric, precipitation, and vegetation dynamics in Portugal

Diana L. Thatcher [a,*], Alan D. Wanamaker [a], Rhawn F. Denniston [b], Caroline C. Ummenhofer [c], Frederico T. Regala [d,e], Nuno Jorge [f], Jonathan Haws [e,g], Alaina Chormann [h], David P. Gillikin [h]

[a] Department of Geological and Atmospheric Sciences, Iowa State University, Ames, Iowa 50011, USA
[b] Department of Geology, Cornell College, Mount Vernon, Iowa 52314, USA
[c] Department of Physical Oceanography, Woods Hole Oceanographic Institution, Woods Hole, MA 02543, USA
[d] Associação de Estudos Subterrâneos e Defesa do Ambiente, Torres Vedras, Portugal
[e] Interdisciplinary Center for Archaeology and Evolution of Human Behaviour (ICArEHB), Universidade do Algarve, Faro, Portugal
[f] Grutas de Mira de Aire, Mira de Aire, Portugal
[g] Department of Anthropology, University of Louisville, Louisville, KY 40208, USA
[h] Department of Geology, Union College, Schenectady, NY 12308, USA

ARTICLE INFO

Editor: Michael E. Boettcher

Keywords:
Karst
Vegetation
Azores High
NAO
Precipitation
Isotopes
Cave monitoring
Portugal

ABSTRACT

Cave deposits can be valuable sources of paleoclimate data, especially when atmospheric circulation patterns, precipitation variability, vegetation changes, and the chemical evolution of waters moving through the karst environment can be mechanistically linked to speleothem proxies. In particular, an evaluation of the factors that control the isotopic composition of precipitation and the evolution of rainwater during migration from the land surface to the cave are needed to robustly develop speleothems as hydroclimate-sensitive proxies. One area in which precipitation and atmospheric variability are closely linked is western Iberia, where rainfall is strongly influenced by the Azores High, part of the North Atlantic Oscillation (NAO) dipole. Therefore, in order to better characterize the factors that influence the isotopic composition of precipitation in Portugal and to evaluate the potential of using stalagmites from this region as hydroclimate (and NAO-sensitive) proxies, we investigated Global Network of Isotopes in Precipitation (GNIP) data from ten mainland Portugal sites spanning multiple decades. In addition, we use more than one hydrologic year of precipitation amount and isotope data from Buraca Gloriosa (BG), a cave in western Portugal, the site of on-going speleothem analyses, as well as six years of environmental monitoring from BG. We present an integrated analysis of rainfall and vegetation through the normalized difference vegetation index (NDVI) following extremely wet and dry winters. Summer vegetation density, related to the amount of precipitation in the preceding winter wet season, as well as prior calcite precipitation (PCP), would largely control the stable carbon isotopic signature ($\delta^{13}C$) in stalagmites at BG. Cool season recharge is likely the dominant factor for the oxygen isotopic composition ($\delta^{18}O$) of water percolating through the cave system, while amount effects exert the primary control on precipitation $\delta^{18}O$ values. Based on HYSPLIT modeling, moisture sources overwhelmingly originate from the Atlantic Ocean as opposed to the Mediterranean or elsewhere; thus, variability in $\delta^{18}O$ values in the precipitation (and, thus, by inference, those of the dripwater and stalagmites) are primarily reflecting changes in precipitation amount and not changing temperatures or source regions. Together these data constitute an important analysis of the controls of isotope proxies in Portuguese cave systems.

1. Introduction

Karst environments offer a host of possibilities for studying past environments (Fairchild and Baker, 2012). In particular, speleothems (particularly stalagmites) have been used widely to reconstruct past hydroclimate (Asmerom et al., 2020; Ait Brahim et al., 2018; Cheng et al., 2016; Mattey et al., 2008; Wang et al., 2005) and environmental change (Allan et al., 2015; Fairchild and Treble, 2009). Although many

* Corresponding author.
E-mail address: thatcher@iastate.edu (D.L. Thatcher).

https://doi.org/10.1016/j.chemgeo.2020.119949
Received 20 May 2020; Received in revised form 29 September 2020; Accepted 18 October 2020
Available online 29 October 2020

studies (e.g., Martín-Chivelet et al., 2011; Treble et al., 2003) have illustrated how the isotopic and elemental chemistries from speleothems reflect climate external to cave environments, for new cave sites it is important to demonstrate how the karst record is related to and influenced by local and regional processes. Western Portugal is heavily influenced by ocean conditions and atmospheric circulation, most notably the North Atlantic Oscillation (NAO) and is thus suitable for developing paleoclimate reconstructions which may aid in the understanding of the role of the North Atlantic Ocean and NAO, as well as other potential drivers of Iberian climate.

The NAO index is a measure of the pressure gradient between the Azores High (AH) and the Icelandic Low (van Loon and Rogers, 1978), and there is a strong link between NAO phases (NAO+ and NAO-) and changes in storm tracks over the North Atlantic, especially in the winter (Osborn et al., 1999; Serreze et al., 1997; Trigo et al., 2002; Ulbrich and Christoph, 1999). During NAO+ conditions, the difference in sea level pressure (SLP) between the Azores and Iceland is enhanced, and this steep pressure gradient as well as the clockwise rotation of high pressure systems in the northern hemisphere steers storm tracks north of Iberia as a result of atmospheric blocking over Portugal. NAO- conditions are indicative of a more relaxed pressure gradient between the Azores and Iceland and allow storms to track further south, crossing the Iberian Peninsula. These resulting changes in storm track location impact rainfall amounts in many parts of western Europe, including Portugal, and the NAO index is strongly inversely correlated with Portugal precipitation (i.e., higher NAO index means lower Portugal precipitation) and other locations in Iberia (Andreo et al., 2004; Mattey et al., 2008; Xoplaki et al., 2004). As the southern node of the NAO, the AH has a dominant influence on Portugal's weather and climate (Davis et al., 1997). When considering just the AH, it is important to note that the structure (intensity, size, mean location) of the AH strongly impacts precipitation dynamics in this region (Sáez de Cámara et al., 2015). When AH SLP is higher, precipitation in Portugal and much of the Iberian Peninsula is reduced, and thus hydroclimate-sensitive proxies from this region have the potential to elucidate not only past precipitation patterns but regional atmospheric dynamics as well.

Although modern relationships among the NAO, AH, and Portuguese precipitation are fairly well understood (Trigo et al., 2004), less is known about the persistence and robustness of these relationships in the past. Thus, speleothem records of hydroclimate from this area are of particular value, including those from Buraca Gloriosa (BG) cave. The goal of this study is to better understand the climatic origins of carbon and oxygen isotopic variability in speleothems from western Portugal and specifically BG cave, and toward this end, we have conducted a novel and detailed assessment of the controls on isotopes in precipitation, the links between precipitation and vegetation, and the way in which these signals are transmitted to cave dripwater.

1.1. Linking geochemical signatures in speleothems to the environment

1.1.1. Oxygen isotopes ($\delta^{18}O$) and the global network of isotopes in precipitation (GNIP) database

An understanding of the dominant drivers of oxygen isotopes in precipitation is required for a robust paleoclimatic interpretation of oxygen isotopes in speleothems. The oxygen isotopic composition ($\delta^{18}O$) of precipitation reflects the influences of many factors including altitude, distance from the ocean, amount of precipitation, surface air temperature, and moisture source, as well as humidity, surface roughness, and wind speed at the point of evaporation (e.g., Dansgaard, 1964). Portugal's varied topography (altitude range 0–1993 m) and latitudinal extent (37.0–42.2°N), both of which impact mean annual temperature (MAT), can impact precipitation $\delta^{18}O$ values. The moisture source region, precipitation amount, and air temperature effects are tested using the set of monitoring data presented here.

Portuguese data from the Global Network of Isotopes in Precipitation (GNIP) are available at 24 locations over much of the last fifty years. Observations from the Azores Islands began in 1962 and from mainland Portugal in 1978 with additional observations coming from the Madeira Islands beginning in 1988 (IAEA/WMO, 2020). Previous work with precipitation isotopes from Iberia include that of Carreira et al. (2005), which used seven mainland Portugal stations plus Lisbon data to look at monthly (all locations) and daily (Lisbon) events and that of Araguas-Araguas and Diaz Teijeiro (2005), which characterized oxygen isotopes from the entire Iberian Peninsula using monthly data from seven mainland Portugal locations plus 16 locations in Spain. A more comprehensive analysis that includes the most recent data and from all ten mainland GNIP stations is lacking. GNIP data from Portugal are useful for characterizing broad influences on precipitation isotopes and, when paired with site-specific precipitation analysis, such as performed in this study for BG, allows for a critical evaluation of the factors controlling the $\delta^{18}O$ signature of dripwater and that of stalagmite $\delta^{18}O$ calcite from a particular site, such as BG cave.

1.1.2. Stable carbon isotopes ($\delta^{13}C$)

The origins of carbon isotopic variability in speleothems can reflect the complex interactions of a wide array of factors. The three main sources of carbon, although not necessarily equal in their contribution, in speleothems are: i) atmospheric CO_2, ii) CO_2 produced from soil microbial respiration (i.e., soil atmosphere), and iii) carbonate ($CaCO_3$) bedrock hosting the cave (Cosford et al., 2009; Fohlmeister et al., 2020; Genty et al., 2003; Hendy, 1971). As rainwater falls, atmospheric CO_2 is dissolved in rainwater to form carbonic acid (H_2CO_3). Microbial processes within the vegetation and soil overlying the bedrock may, in all but thin and vegetation-poor soils, produce CO_2 at levels that overwhelm atmospheric CO_2. The resulting carbonic acid is primarily responsible for the dissolution of the carbonate limestone bedrock (Baldini et al., 2006).

The conditions under which dissolution proceeds (open, closed, or intermediate) impacts the carbon isotopic composition ($\delta^{13}C$) of seepage water dissolved inorganic carbon (DIC; Dulinski and Rozanski, 1990; Hendy, 1971; Salomon and Mook, 1986). In an open system, percolating fluid exchanges with soil CO_2 until degassing occurs in the cave. In this system, the $\delta^{13}C$ of the DIC is dominated by the soil CO_2 (Fohlmeister et al., 2011), which is overwhelmingly determined by photosynthesis and respiration (Genty et al., 2006; Meyer et al., 2014). In a closed system, CO_2 is isolated from soil gases once it enters the bedrock (Hendy, 1971); hence, the $\delta^{13}C$ of the seepage DIC depends on both the soil $\delta^{13}C$ of CO_2 and the $\delta^{13}C$ of limestone (McDermott, 2004). Drier and wetter conditions could lead to shifts between open and closed system behavior, respectively, and the shifts in isotopic values that result from shifts between open and closed system behaviors has been considered (e.g. Fohlmeister et al., 2011; Hendy, 1971).

Based on these processes, $\delta^{13}C$ values from speleothems may be useful to assess paleohydroclimate. The $\delta^{13}C$ of atmospheric CO_2 prior to 1850 CE was approx. -6.4‰ (Francey et al., 1999), while CO_2 produced by soil respiration reflects that of vegetation (−12 to −27‰, depending on vegetation type) (Cerling, 1984; Deines, 1980; O'Leary, 1988; Von-Fischer et al., 2008). The soil CO_2 concentration changes with depth below the land surface due to diffusion processes between the soil and atmosphere that results in lower soil gas $\delta^{13}C$ values in deeper depths. During wetter conditions, as vegetation density and soil microbial activity increase, the amount of soil CO_2 increases and the $\delta^{13}C$ values of soil CO_2 decrease (Cerling, 1984; Hou et al., 2003; Wainer et al., 2009). A drier climate leads to less vegetation, a reduction in microbial activity, and less soil CO_2 production, which lead to increasing soil CO_2 $\delta^{13}C$ values (Cosford et al., 2009; Genty et al., 2003; Osterlin, 2010; Wainer et al., 2009). However, even if vegetation density was less developed under sustained dry conditions, the contribution of soil CO_2, albeit less pronounced, would modulate the increase in $\delta^{13}C$ values. Additionally, during dry conditions, greater proportions of bedrock may be dissolved by percolating waters, leading to higher dripwater $\delta^{13}C$ values (Genty et al., 2003). Lastly, under dry conditions, slower percolation rates can

result in dewatering of voids in the epikarst, providing opportunities for evaporation and/or prior calcite precipitation (PCP) (Baker et al., 1997; Cosford et al., 2009) that lead to increased dripwater $\delta^{13}C$ values.

The vegetation response to rainfall amount in Portugal has been investigated in light of the NAO's impact on precipitation (Vicente-Serrano et al., 2011). This is important because the density of the vegetation in karst environments has direct impacts on the processes that influence the carbon isotopic signature of the DIC pool in soil that infiltrates the limestone and eventually form speleothems. In Mediterranean climates such as western Portugal, vegetation density increases in summers following relatively wet winters, and diminishes following relatively dry winters, and in this region, precipitation dynamics are strongly influenced by phases of the NAO (Gouveia and Trigo, 2011). In other words, if the NAO was in a negative phase for several years or more, then vegetation density should increase across the region (and vice versa), as has been explored in Portugal. For example, Vicente-Serrano and Heredia-Laclaustra (2004) demonstrated that certain portions of the Iberian Peninsula (BG cave included) have a negative correlation with annual NDVI and winter NAO (higher NAO and lower precipitation correlated with lower NDVI); Gouveia et al. (2008) indicate that positive values of NAO lead to lower vegetation activity in the spring and summer seasons that follow. Hypotheses of how such vegetation variations would impact the stable carbon isotopic DIC, and thus speleothem values, are outlined in the following paragraph. Across Iberia, differences in topography and proximity to the Atlantic Ocean and Mediterranean Sea cause substantial variability in rainfall patterns and temperature patterns and thus between paleoclimate records. Paleoclimate records from Iberia, some reaching to the present, include lake and marine sediments (Jambrina-Enríquez et al., 2014; Pla and Catalan, 2005; Pla-Rabes and Catalan, 2011; Sánchez Goñi et al., 2008; Sánchez-López et al., 2016) and cave speleothems (e.g., Martín-Chivelet et al., 2011; Smith et al., 2016; Stoll et al., 2013). Additional high-resolution records from this region will allow for a greater understanding of regional climate variability and an evaluation of past hydroclimate variability. This is especially important considering that the Iberian Peninsula is projected to be disproportionally impacted by future warming, likely causing extreme water scarcity issues (Sanchez et al., 2011).

In order to study the dominant factors that influence the isotopic composition of precipitation in Portugal and to evaluate the potential utility of stalagmites as hydroclimate proxies at BG and other regional caves, GNIP data from 10 mainland Portugal sites were investigated. Additionally, we present approximately six years of detailed cave monitoring from BG cave as well as 15 months of precipitation data near and at BG, coupled with Hybrid Single Particle Lagrangian Integrated Trajectory (HYSPLIT) modeling to evaluate moisture sources to BG. The

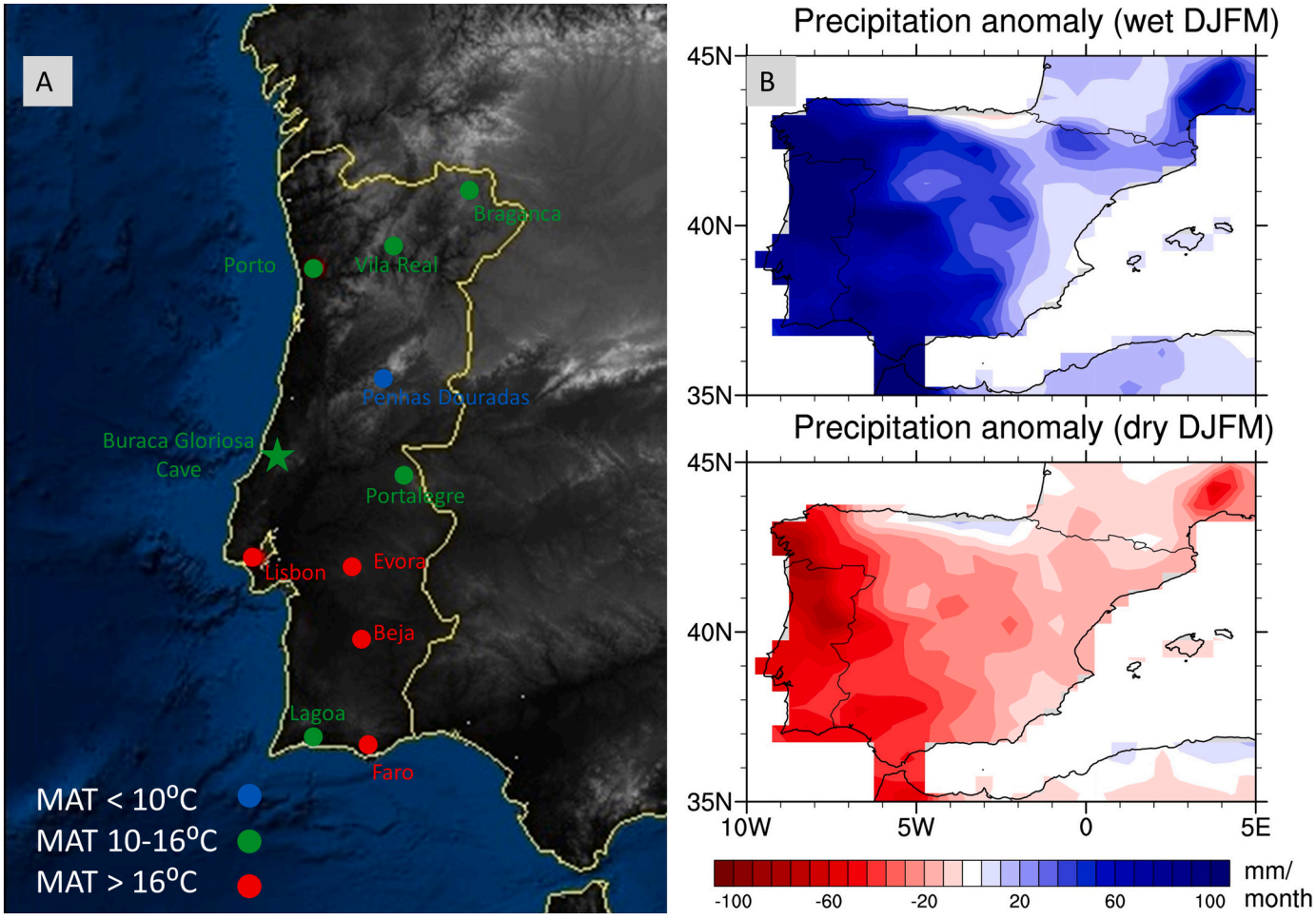

Fig. 1. A. Map of Portugal indicating the ten IAEA Global Network of Isotopes in Precipitation (GNIP) sites discussed in this study. Blue dot indicates location with mean annual temperature (MAT) less than 10 °C. Green dots indicate sites with MAT 10–16 °C and red dots indicate locations with MAT >16 °C. Buraca Gloriosa (BG) cave indicated by green star with MAT between 10 and 16 °C. B. Precipitation anomalies associated with NAO- (top, NAO indices = −1.01, −1.44, −2.57 from 2000-01, 1995-96, and 2009-10, respectively) and NAO+ (bottom, NAO indices = +0.36, +1.29, +1.60 from 2004-05, 1982-83, 2011-12, respectively) conditions. Precipitation anomalies are based on the GPCC precipitation version 7 at 0.5^0 spatial resolution (Schneider et al., 2014). (For interpretation of the references to colour in this figure legend, the reader is referred to the web version of this article.)

length of monitoring paired with GNIP data from mainland Portugal and HYSPLIT modeling of precipitation events allows for the characterization of the recent hydroclimate in western Portugal and the BG cave system. This study also investigates the role of atmospheric and precipitation dynamics on vegetation density to evaluate the reliability of using speleothem $\delta^{13}C$ values to infer vegetation density above the BG cave system. A novel pairing of these techniques allow for a comprehensive analysis of suitability of BG cave for paleoclimate reconstructions and for using stalagmites from BG to analyze hydroclimate and atmospheric dynamics in western Portugal from past glacial conditions, through the Holocene, until modern conditions.

2. Regional setting and site description

2.1. Buraca Gloriosa

Buraca Gloriosa cave (39°32′N, 08°47′W; 420 m a.s.l.) is located in western Portugal near the town of Alvados, 30 km from the Atlantic Ocean and approximately 100 km north of Lisbon (Fig. 1). The cave is ~35 m-long and formed in Middle Jurassic limestone in the Estremadura Limestone Massif, a topographically distinct region in central Portugal (Rodrigues and Fonseca, 2010). While not deep, air exchange in the cave is limited by the single, small (~0.5 m^2) entrance that is accessed near the top of a ~ 30 m escarpment and that leads through a collapse into the upper end of the downward-sloping cave. The entrance is shielded from the external environment by the surrounding boulders and trees. BG is well-decorated with numerous inactive stalagmites but few active growth sites. Of particular interest in the cave is the loft, an elevated and somewhat secluded area at the rear of the cave and the location of several actively growing stalagmites (Thatcher et al., 2020). Vegetation above the cave is composed of shrubs, small trees, and mosses with thin (0-10 cm), highly organic soil (Fig. 2). Although there has been mining in the region, there is no evidence of alteration above the cave.

The region surrounding BG is characterized by the warm, dry summers and cool, wet winters typical of Mediterranean climate. Most rainfall occurs in the winter season and shoulder months, with greater than 85% of annual precipitation falling between October and April in Leiria, a meteorological station less than 30 km north of BG (Fig. S1).

3. Methods

3.1. Global network of isotopes in precipitation (GNIP) database

The GNIP data used in this study were collected monthly at ten locations in mainland Portugal: Beja (1988–1991), Bragança (1988–1991), Evora (2014–2017), Faro (1978–2001), Lagoa (2014–2017), Lisbon (2003, 2014–2017), Penhas Douradas (1988–2004), Portalegre (1988–2004), Porto (1988–2004, 2014–2017), and Vila Real (1988–1991) (IAEA/WMO, 2020; Fig. 1). Together, these constitute 905 months of observations of monthly average temperature, monthly total precipitation amount, and oxygen and hydrogen isotopes of the bulk monthly precipitation. The relationships between amount weighted $\delta^{18}O$ and latitude, altitude, temperature, and precipitation amount were determined using these observations. In particular, amount-weighted $\delta^{18}O$-temperature and amount-weighted $\delta^{18}O$-precipitation amount were explored as amount-weighted monthly averages from each location, and then also for three separate bins of mean annual temperature (MAT).

3.2. Atmospheric, precipitation, and vegetation index datasets

Winter (December–January-February-March; DJFM) NAO index

Fig. 2. Buraca Gloriosa cave site. A. Image of vegetation growing above BG cave. B. Typical soil above BG cave. C. Shallow soil cover above cave.

values were obtained using the Hurrell Principal Component-based (PC-based) index (Hurrell, 1995; Hurrell and Deser, 2009; NCAR, 2019). We selected the PC-based record to account for non-stationarity of the NAO system; the Hurrell PC-based monthly dataset is the average monthly NAO index and spans the period 1899–2015.

Monthly gridded precipitation data were used from the Global Precipitation Climatology Centre (GPCC), version 7, at 0.5° horizontal resolution and available for the period 1901–2013 (Schneider et al., 2014).

We also utilized a daily rainfall series from 1864 to 2013 at the D. Luis observatory (38.72°N, 9.15°W; 95 km south of BG) (Kutiel and Trigo, 2014). The three highest and three lowest precipitation winters (DJFM) from 1982 to 2013 were selected for analysis. The SLP dataset used here is from Ponte Delgado, Azores and is monthly averaged SLP for all months 1874–2005 (polarmet.osu.edu/NAO). Correlations were determined between Lisbon daily rainfall (aggregated into monthly totals), Ponte Delgado monthly SLP data, and Hurrell PC-based NAO index.

Vegetation density was obtained using the normalized difference vegetation index (NDVI), which has been measured globally since 1982 and is one of the most used indices to detect live green plant canopies (Karnieli et al., 2010; NCAR, 2018; Tucker, 1979). Values range from −1.0 to +1.0 with higher values suggesting greater biomass and enhanced plant vigor. The vegetation index for the Iberian Peninsula was acquired using the Advanced Very High Resolution Radiometer (AVHRR) sensor with a grid size of 0.05° x 0.05°, at daily resolution, and covering the period 1981-present. The NDVI was averaged for the summer months (June–July-August; JJA) following the wettest and driest winters for the Iberian Peninsula: for example, DJFM 2009–2010 was the wettest winter since 1982 and the NDVI was determined for JJA 2010.

3.3. Rainfall and dripwater isotopes and speleothem drip rates at BG

Measurements of rainfall totals were obtained at Leiria and Monte Real, approximately 30 km and 50 km north of BG, respectively. Rainwater samples were collected over fifteen months (September 2018 – November 2019) on any day that precipitation fell at Mira de Aire, a tourist cave approx. 5 km from BG cave.

Additionally, a Pluvimate (http://www.driptych.com) automated rain gauge was installed outside of BG in September 2018 to compare rainfall amounts at the cave entrance to the other collection/measurement sites (Leiria, Monte Real, and Mira de Aire). Integrated rainfall at this site was collected using a Palmex rain sampler (http://www.rainsampler.com/) for four periods: September 2018–January 2019, January 2019–June 2019, June 2019–August 2019, and August 2019–December 2019 and analyzed for oxygen and hydrogen isotopes.

Drip rates were measured at two locations within the loft beginning June 2014. Drip rates were logged every thirty minutes using Stalagmate acoustic drip loggers (http://www.driptych.com; Collister and Mattey, 2008; Smith et al., 2016). An additional drip counter was installed in September 2018 at the base of the loft area. Daily drip rates were calculated for a total of 54 months over the 62-month time period June 2014 to August 2019. The drip counters were removed for a several month time period in 2016 and drip counters failed to measure drips during other time periods, likely due to shifting drip position.

BG dripwater was collected sporadically in two ways: months-long integrated sampling and drips obtained over several minutes during monitoring visits (June 2014, November 2014, October 2015, March 2016, January 2018, September 2018, January 2019, June 2019, August 2019, and December 2019). For the present study, a total of 42 dripwater samples were analyzed for isotopes. Drips were primarily obtained from two areas in the cave: the loft and along a flowstone wall directly under the loft.

$\delta^{18}O$ and stable hydrogen isotopes ($\delta^{2}H$) values of all rainwater and dripwater were analyzed with a Picarro L1102-i Isotopic Liquid Water Analyzer with autosampler and ChemCorrect software at Iowa State University. Each sample was measured six times, with only the last three injections used to determine isotopic values in order to minimize memory effects. Three reference standards (VSMOW, IAEA-OH-2, IAEA-OH-3) were used for regression-based isotopic corrections and to assign the data to the appropriate isotope scale. Reference standards were measured at least once every five samples. The analytical errors reported at one standard deviation are, on average, better than 0.1‰ (1σ) for $\delta^{18}O$ and 0.2‰ (1σ) for $\delta^{2}H$ and are reported relative to VSMOW.

3.4. Evaluating moisture source dynamics at Buraca Gloriosa

The influence of atmospheric trajectory (moisture source) on western Portugal rainfall isotopic composition was studied by integrating rainwater isotopes and HYSPLIT modeling (Draxler and Hess, 1998; Draxler and Rolph, 2003) using the methods of Baldini et al. (2010) and Smith et al. (2016). The air mass history of each rainfall event was calculated at three heights (1500, 3015, and 5575 m), roughly corresponding to 850, 700, and 500 mb, using five-day (120h) kinematic back trajectory modeling from BG. The 850 and 700 mb heights were used for modeling to approximate frontal and synoptic rainfall. The 500 mb level was not used to identify moisture source regions but provided a check for atmospheric shear (Baldini et al., 2010). The models originate at 09:00 local time, the time rainwater was collected at Mira d'Aire. Samples encompass the entire rainfall collection day (24 h prior to 09:00 local time), and average source directions were calculated for each precipitation event using the 120 h of data.

3.5. External and internal cave monitoring

External and cave air temperature and relative humidity were measured every 30 min using HOBO U23 loggers. In August 2013, one data logger was installed directly outside the cave entrance and adjacent to the cliff wall, and in September 2018, an additional logger was installed in an area with adequate ventilation at a height of 1 m above the ground located in a small clearing several meters from the cave entrance. Logging of cave temperature was conducted at several locations, with all loggers suspended approximately 1 m above the cave floor and not touching the side walls of the cave. Data presented here were obtained near the loft in the rear of the cave. Dripwater temperatures have been recorded every 30 min in the loft since August 2016 using a HOBO Tidbit UTBI-001 logger. Cave air pressures have been recorded every two hours since August 2013 and external air pressures every hour since September 2018 using HOBO U20 loggers.

4. Results

4.1. Evaluation of the global network of isotopes in precipitation (GNIP) in Portugal

The mainland Portugal GNIP database contains 905 months of overlapping data, with $\delta^{18}O$ and $\delta^{2}H$ values ranging from −14.7 to +1.1‰ and − 106.1 to +36.7‰, respectively. Regressing all of the Portugal GNIP data yields a local meteoric water line (LMWL) of $\delta^{2}H = 6.72*\delta^{18}O + 4.39$ (Fig. 3A). Additionally, data from Mira de Aire precipitation alone produces a LWML of $\delta^{2}H = 7.16*\delta^{18}O + 10.90$. Both the mainland Portugal LWML and Mira de Aire LMWL have lower slopes than the Global Meteoric Water Line (GMWL; $\delta^{2}H = 8*\delta^{18}O + 10$; Craig, 1961), the mainland Portugal LWML intercept is lower than that of the GWML, and the Mira de Aire LMWL has an intercept similar to that of the GWML (Fig. 3).

For the mainland Portugal GNIP data, comparisons were made with $\delta^{18}O$ values and latitude, altitude, mean annual temperature, and average annual precipitation for the ten locations (Fig. 4). Across all of Portugal, the strongest relationship was between annual precipitation $\delta^{18}O$ values and altitude ($r^2 = 0.92$, $p < 0.05$; slope = −0.24‰/100 m),

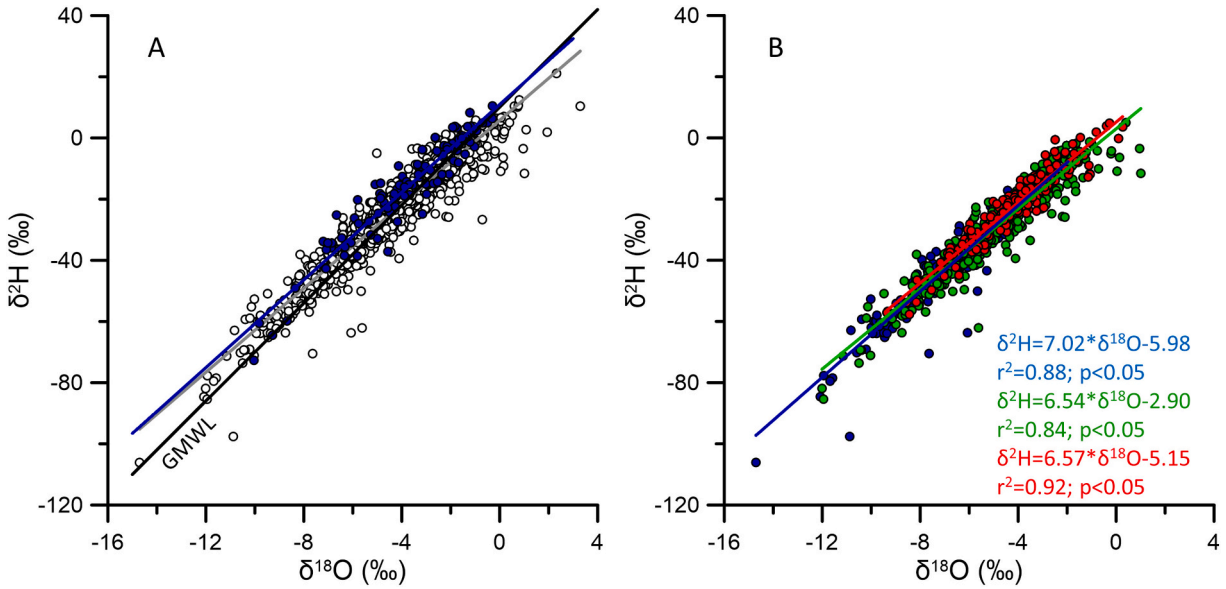

Fig. 3. A. All mainland Portugal GNIP data (unfilled circles) with Mira de Aire precipitation data (blue). Also shown GMWL (black line), all Portugal GNIP LMWL (gray line), and Mira de Aire LMWL (blue line). B. All Portugal GNIP separated by mean annual temperature (MAT). Circles are individual monthly precipitation samples (MAT >16 °C, red; 10 °C < MAT <16 °C, green; MAT <10 °C, blue). Individual LMWL are plotted for the three MAT bins along with LMWL equations, r^2 values and *p*-values. (For interpretation of the references to colour in this figure legend, the reader is referred to the web version of this article.)

followed by monthly average precipitation $\delta^{18}O$ values and monthly precipitation amount ($r^2 = 0.28$, $p < 0.05$, slope = −1.8‰/100 mm precip), and monthly average precipitation $\delta^{18}O$ values and mean annual temperature ($r^2 = 0.22$, $p < 0.05$; slope = +0.16‰/°C). The weakest relationship between annual precipitation $\delta^{18}O$ values is latitude ($r^2 = 0.22$, $p = 0.17$; slope = −0.29‰/degree latitude) and this relationship is not statistically significant. These relationships are based on the amount-weighted mean $\delta^{18}O$ values calculated for each of the ten mainland Portugal locations using a total of 832 months for precipitation amount and 667 months for temperature values (data not available for all months at every location) across all years and locations. However, it may not be useful to assess these relationships across the entirety of Portugal as one dataset because of the inherent differences in climatic zones. For example, Baker et al. (2019) demonstrated that regions with different mean annual temperatures (MATs) would have differing dominant controls on $\delta^{18}O$ values of precipitation. Hence, we regressed the GNIP data binned by MAT to produce three new LMWLs (Fig. 3B) and determined relationships with the $\delta^{18}O$-precipitation amount and $\delta^{18}O$-temperature (Table 1). The slope and intercept for the LWML for each are as follows: MAT >16 °C (6.57, 5.15), 10 °C < MAT<16 °C (6.54, 2.90), and MAT <10 °C (7.02, 5.98). When considering the relationships between amount weighted $\delta^{18}O$-precipitation amount and amount weighted $\delta^{18}O$-temperature with respect to the three MAT bins, the relationships that are statistically significant (bold in Table 1) are those records that are longer and/or those from regions with MAT <16 °C, with the exception of Vila Real. All of the longer records (> 4 years) have statistically significant relationships with both $\delta^{18}O$-precipitation amount and $\delta^{18}O$-temperature. For three of the four longer records, the r^2 value is higher for the precipitation amount relationship. Additionally, two other locations with MAT 10–16 °C (Bragança and Lagoa) have statistically significant relationships with $\delta^{18}O$-precipitation amount but not with temperature.

4.2. Atmospheric, precipitation, and vegetation index datasets

The three lowest and highest DJFM rainfall totals during 1982–2018 (the length of the NDVI record) were determined and compared with the NAO index. The three wettest winters were 2000–01 (720.8 mm, NAO index = −1.01), 1995–96 (789.4 mm, NAO index = −1.44), and 2009–10 (984.3 mm, NAO index = −2.57). The three driest winters were 2004–05 (77.7 mm, NAO index = +0.36), 1982–83 (82.4 mm, NAO index = +1.29), and 2011–12 (102.2 mm, NAO index = +1.60). For each of the six years, average summer NDVI values were determined and then a composite formed for the three years with driest and wettest conditions, respectively, and shown across the entire Iberian Peninsula (Fig. 5). Higher NDVI (more vegetation) are in green and lower NDVI (less vegetation) in brown. There are considerable differences in vegetation density for individual summers following either wet or dry winters (Fig. 5). However, when several wet (Fig. 5B) or dry (Fig. 5D) years are averaged, a general response to the vegetation density emerges. For example, by subtracting the composite average NDVI during dry years from that of the wet years at each grid point (Fig. 5E) the impact on vegetation density can be easily seen. NDVI values for a 1°x1° grid box (8–9°N, 39–40°W, box shown in Fig. 5E) for summers following the wettest winters averaged 0.404, while they averaged 0.337 following the driest winters There is spatial variability in the difference between the wettest and driest years (Fig. 5E). For example, parts of northern Spain show little difference in vegetation between these wet and dry years while most of western Iberia shows substantial differences in NDVI between wet and dry years. In the grid box, the difference in NDVI between the wettest and driest years is 0.0668, one of the largest differences in Iberia. This result indicates that western Portugal has a higher vegetation density following wet winters/NAO- years and a lower vegetation density following dry winters/NAO+ years.

4.3. Rainfall and dripwater isotopes and speleothem drip rates at BG

In order to develop a comprehensive rainfall record for the period of study, we utilize six years of rainfall totals at the Leiria and Monte Real stations (Fig. S1). Because neither record is continuous over this time period, we combine the two locations. Annual average rainfall was 594 mm/yr at Leiria (30 km from BG; 2015–2018) and 487 mm/yr at Monte Real (50 km from BG; 2014–2018). A comparison of rainfall data from Leiria, Monte Real, and Mira de Aire, and rainfall from the Pluvimate outside BG for the period September 2018–August 2019 is shown in Supplemental Fig. S1.

At Mira de Aire, 108 precipitation days occurred from September 2018–November 2019, with precipitation totals ranging from 0.1 to

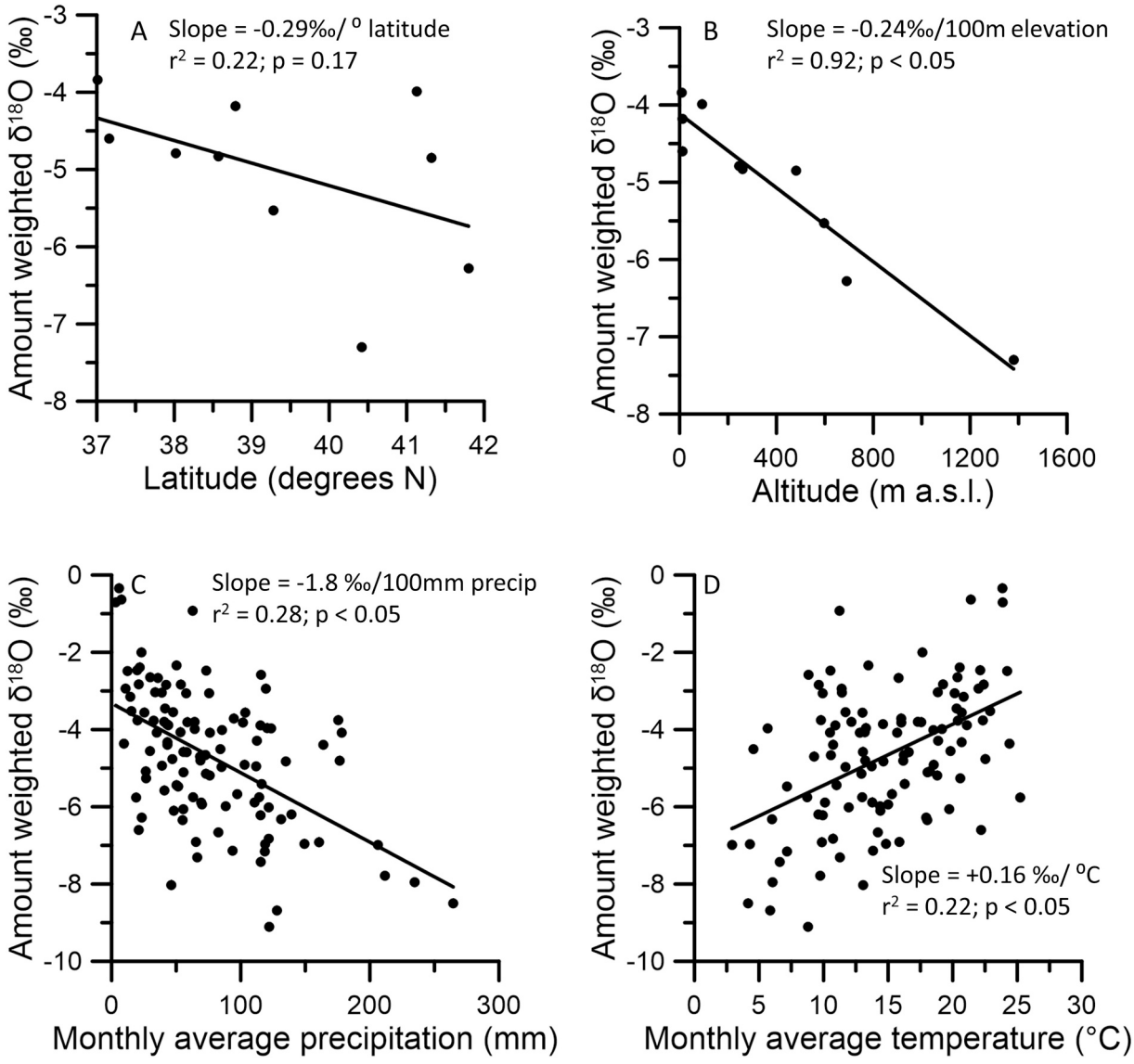

Fig. 4. Amount-weighted $\delta^{18}O$ values from ten locations across mainland Portugal compared to A. Latitude, B. Altitude, C. Monthly average precipitation amount, and D. Monthly average temperature.

Table 1
Portugal mainland GNIP data. Relationships between weighted $\delta^{18}O$ values and precipitation (middle column) and weighted $\delta^{18}O$ values and temperature (right column). Significant relationships are in **bold.**

		Weighted $\delta^{18}O$ /precipitation			**Weighted $\delta^{18}O$/temperature**		
Site	**Length of Record (years)**	Slope (‰/100 mm/month)	r^2	p-value	Slope (‰/^{0}C)	r^2	p-value
MAT < 10 °C							
Penhas Douradas	17	−1.01	**0.75**	**< 0.05**	0.12	**0.47**	**< 0.05**
10 °C < MAT < 16 °C							
Braganca	4	−4.18	**0.57**	**< 0.05**	0.077	0.056	0.46
Lagoa	4	−2.94	**0.51**	**< 0.05**	0.12	0.32	0.24
Portalegre	17	−1.75	**0.55**	**< 0.05**	0.15	**0.69**	**< 0.05**
Porto	21	−1.04	**0.76**	**< 0.05**	0.11	**0.38**	**< 0.05**
Vila Real	4	−1.90	0.18	0.16	−0.017	0.0025	0.88
MAT > 16 °C							
Beja	4	−2.17	0.21	0.18	0.029	0.0075	0.81
Evora	4	−0.07	0.000038	0.99	0.13	0.12	0.37
Faro	24	−3.78	**0.77**	**< 0.05**	0.31	**0.70**	**< 0.05**
Lisbon	5	−0.44	0.85	0.53	0.011	0.03	0.88

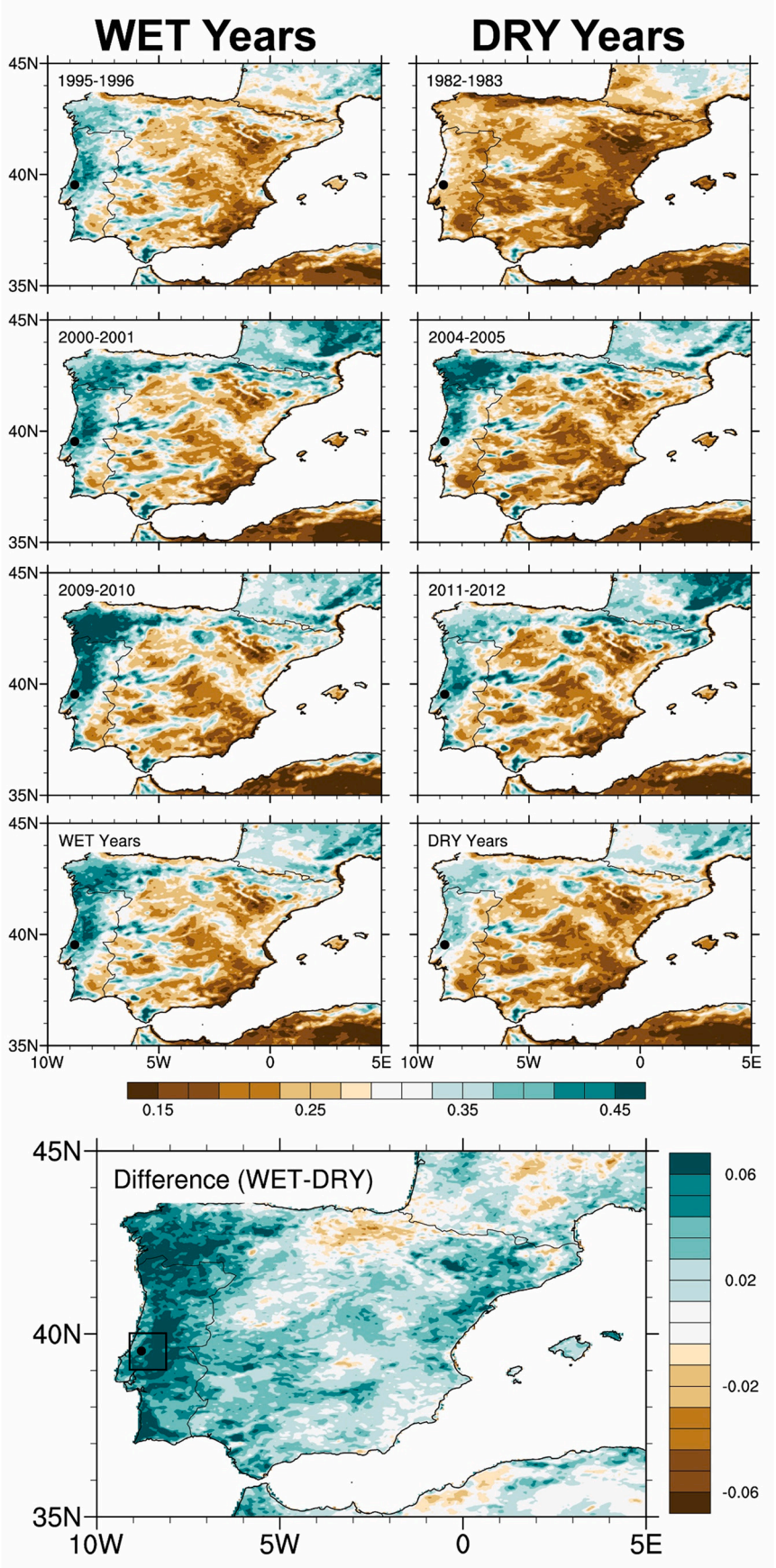

Fig. 5. A. Jun-Aug NDVI following the three highest precipitation Dec-Mar time periods since 1982. B. Jun-Aug composite NDVI following the three highest precipitation Dec-Mar time periods since 1982. C. Jun-Aug NDVI following the three lowest precipitation Dec-Mar time periods since 1982. D. Jun-Aug composite NDVI following the three lowest precipitation Dec-Mar time periods since 1982. E. The bottom plot is the NDVI difference plot of average wet years minus average dry years. Box indicates location of average values of NDVI. Dot on each map indicates BG cave.

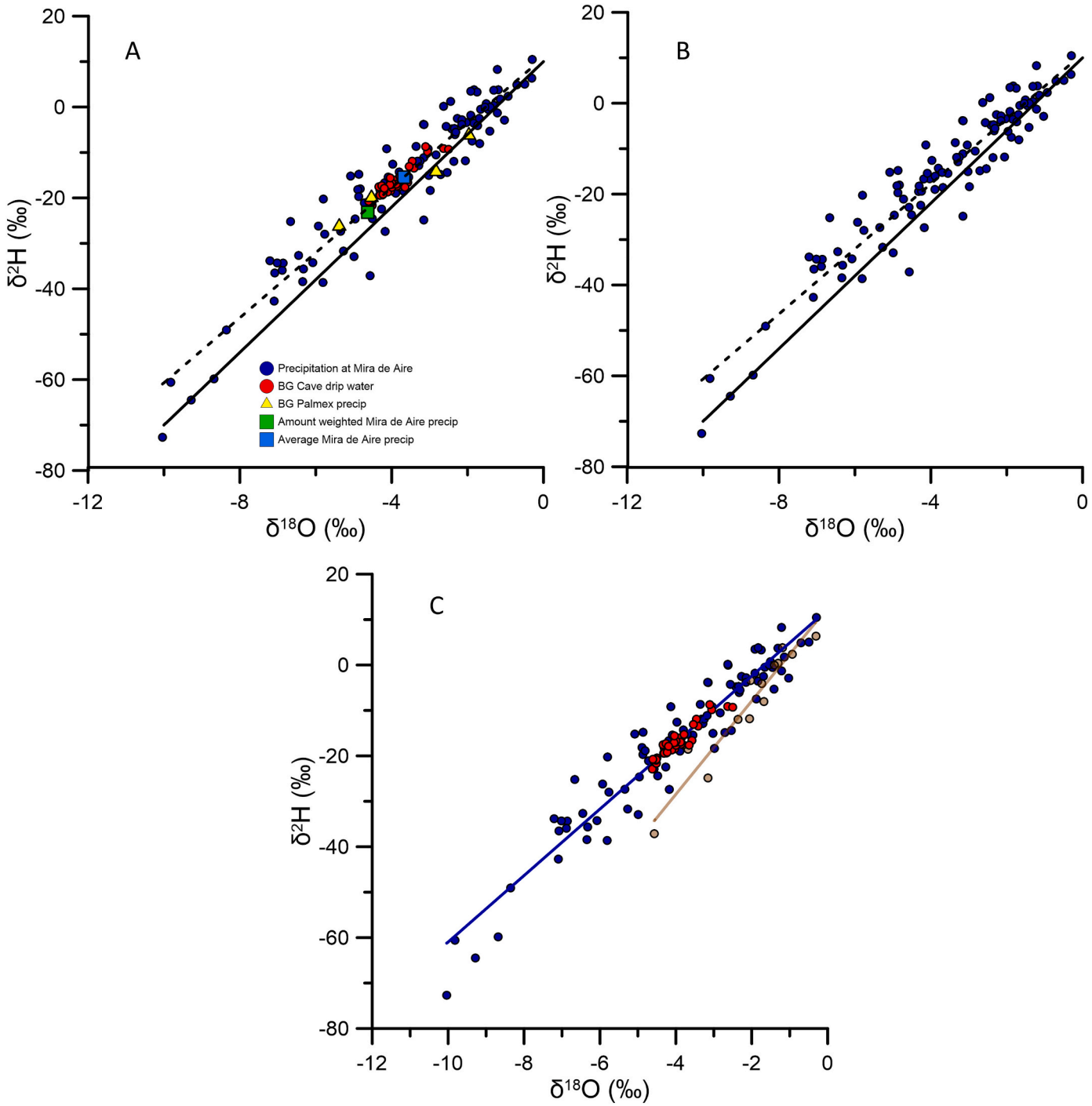

Fig. 6. *A.*Mirade Aire precipitation (blue circles), BG cave drip water (red circles), BG bulk precipitation (yellow triangles), Mira de Aire amount-weighted average precipitation (green square), Mira de Aire average precipitation (light blue square), Mira de Aire LMWL (dashed), and GMWL (solid black). B. Rainfall data from Mira de Aire (~5 km from BG) with LMWL (dashed) and GMWL (solid) shown C. Wet season LMWL (October–April, blue) and dry season LMWL (May–September, brown) with BG cave drip water (red). (For interpretation of the references to colour in this figure legend, the reader is referred to the web version of this article.)

46.0 mm (blue circles in Fig. 6A). The $\delta^{18}O$ and $\delta\ ^{2}H$ values of precipitation collected at this site range from −10.0 to −0.3‰ and − 72.7 to +10.5‰, respectively, with average values of −3.7 (±2.2) ‰ and − 15.5 (± 16.4) ‰ (Fig. 6A). Additionally, four composite samples were collected from the Pluvimate rainfall collector. The $\delta^{18}O$ and $\delta\ ^{2}H$ values for the four composite samples fall within the range of the daily precipitation samples collected at Mira de Aire (Table S1, yellow triangles in Fig. 6A).

Daily rainwater sampling allows for the construction of a local meteoric water line (LMWL). Similar to the Global Meteoric Water Line ($\delta^2H = 8.0*\delta^{18}O + 10$) (Craig, 1961), the Mira de Aire LMWL is defined as $\delta^2H = 7.16*\delta^{18}O + 10.90$ (Fig. 6B) and has a similar slope (but different intercept) to a Western Mediterranean Meteoric Water Line (WMMWL) created by Celle (2000): $\delta^2H = 7.43*\delta^{18}O + 8.06$. Differences in slope are prominent when precipitation samples are segregated into wet and dry seasons. For the wet season (October – April), the Mira de Aire LMWL is $\delta^2H = 7.32*\delta^{18}O + 12.21$ and for the dry season (May – September), the LMWL is $\delta^2H = 10.27*\delta^{18}O + 12.64$ (Fig. 6C).

Dripwater isotopes have an isotopic range of −4.6 to −0.4‰ for $\delta^{18}O$ and − 22.9 to +0.3‰ for $\delta^{2}H$ with average values of −3.8 and − 15.6‰, respectively. Variability among the six dripwater samples is approximately 20% that of the variability in precipitation over the course of one year (see Fig. 6A). Fig. 6A displays the oxygen and hydrogen isotopes from the 108 precipitation events from Mira de Aire, the amount-weighted average (green square) and the average (light blue square) of these 108 samples of precipitation. Overlaid on these precipitation isotopes are 42 samples of dripwater isotopes from BG cave (red circles). A time series of the precipitation isotopes from the 108 events is shown in Fig. S2. The dripwater isotopes are similar to the amount-weighted average $\delta^{18}O$ and $\delta^{2}H$ values from the 108 samples of precipitation collected at Mira de Aire (−4.63 and 23.18‰, respectively).

Drip rates were measured for much of the period spanning June 2014 to August 2019 (for a total of 54 months) and exhibit seasonal variations tied to the winter wet and summer dry seasons, as well as individual rain events (Fig. 7). The three drip counters installed in the cave record different numbers of drips per day but have similar patterns in seasonal fluctuations.

4.4. Moisture source dynamics at Buraca Gloriosa

All precipitation events at Mira de Aire were analyzed by HYSPLIT for the average direction of air mass transport for the 120 h prior to arriving at BG at 850 mb. Average air mass trajectories were compared to precipitation isotopes for each event, with the results shown in Fig. 8. Rainfall from the west and northwest had oxygen isotopic values that ranged from −10.0 to −0.3‰. Of the 108 events, 89% were derived from the Atlantic (average air mass trajectory angles between 180° (from the south) and 360° (from the north)). An additional 5% of precipitation days involved moisture transport from central Europe (average air mass trajectory angles between 1 and 12° (east of north)). This finding also largely holds for the relationship between rainfall amount and average direction of air mass transport. Lightest precipitation events (<10 mm/day; $n = 68$) were predominantly Atlantic but originated from a variety of directions and the largest (>30 mm/day; $n = 4$) were all derived from the Atlantic (270° to 360°).

Additionally, between 1982 and 2018, the three wettest winters in Lisbon (2000–2001, 1995–1996, 2009–2010) contained a total of 230 precipitation days (Fig. 8). During these years, 94% of the events were derived from air mass trajectories between 180° and 360° with an additional 7 events 1–12°. The three driest years in Lisbon (2004–2005, 1982–1983, 2011–2012) recorded 77 precipitation days. During these driest years, 84% of the events had air mass trajectories from the Atlantic (180–360°) with an additional 3 events between 1 and 12°.

4.5. External and internal cave monitoring

External temperatures show diurnal and seasonal variability (3.6 to 31.4 °C; annual mean of 15.4 ± 4.7 °C; Fig. 9) while cave temperatures show little variability throughout the year. Cave temperatures vary from 13.7 to 14.8 °C with warmest temperatures generally occurring October–November and coolest temperatures January–March (Fig. 7). The annual mean temperature inside the cave is 14.3 ± 0.2 °C, approximately 1 °C cooler than the outside temperature measured directly adjacent to the rock (near entrance). This near entrance outside temperature measurement is likely inaccurate and results from the weather station away from the rock will provide increased clarity. However, due to the short nature of the monitoring campaign at the location away from the rock, an annual mean at this location cannot yet be calculated. Dripwater temperatures vary from 13.8 to 15.4 °C, with an average value of 14.3 ± 0.2 °C, identical to the mean annual cave air

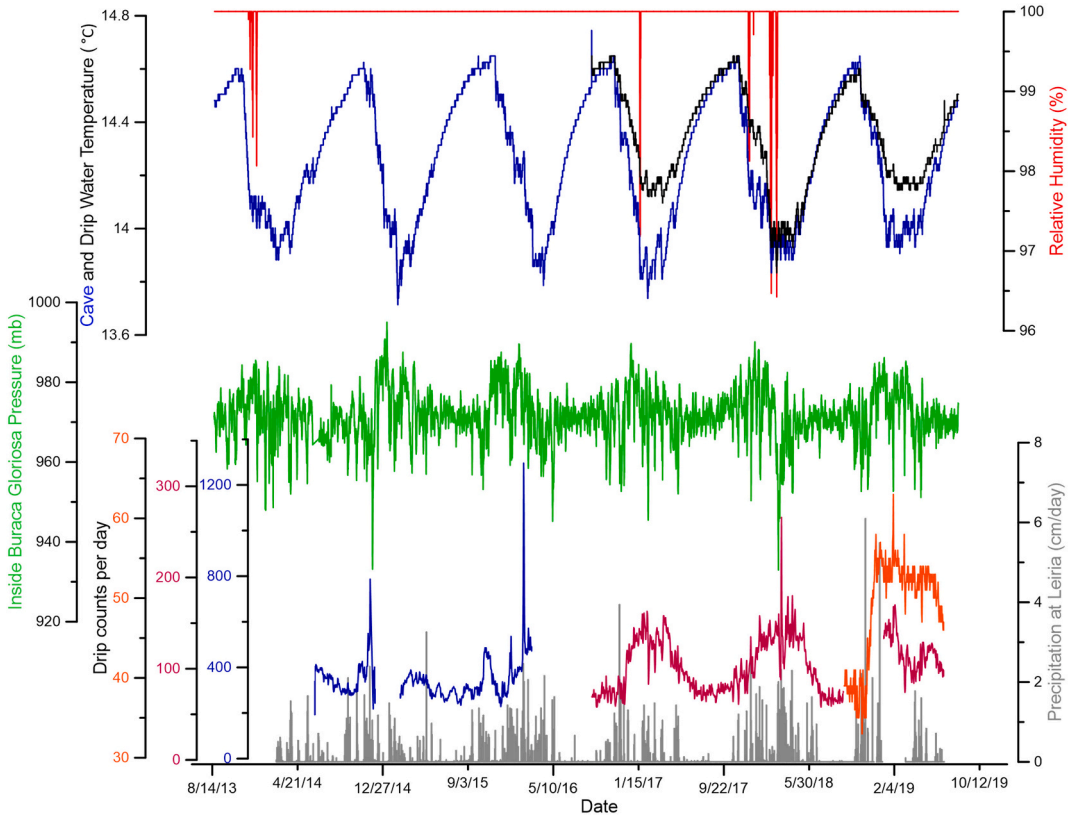

Fig. 7. Environmental monitoring inside BG from August 2013–June 2019. A. Relative humidity (red) from inside BG. B. Cave temperature (blue) and drip water temperature (black) from inside BG. C. Barometric pressure inside BG (green). D. Drip counts from three drip counters located inside BG. E. Precipitation from Leiria (gray; approx. 30 km from BG). (For interpretation of the references to colour in this figure legend, the reader is referred to the web version of this article.)

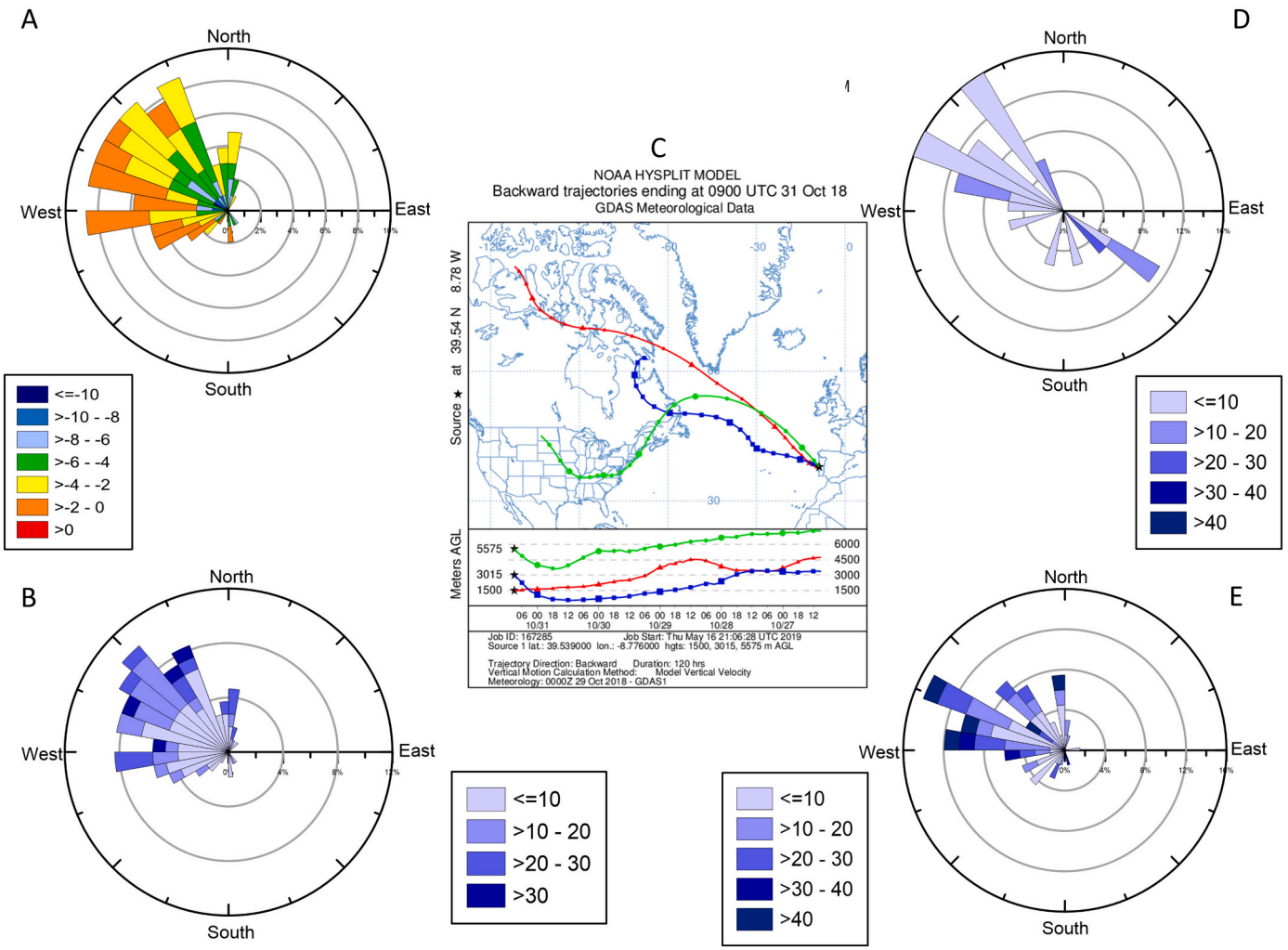

Fig. 8. A. Wind rose plot of moisture transport direction to BG relative to rainfall oxygen isotopes (‰). B. Wind rose plot of moisture transport direction to BG relative to precipitation amount (mm/day). C. Example output from Hysplit model. D. Wind rose plot of moisture transport with the airmass directions from the lowest three precipitation winters since 1982 (mm/day). E. Wind rose plots of moisture transport direction to Lisbon with the airmass directions for the highest three precipitation winters since 1982 (mm/day). For A, B, D, & E, source regions are combined into 5° bins and the % of rainfall from each sector is shown as light gray circles. Moisture transport direction was calculated using the Hysplit Model (Draxler and Hess, 1998), following the methods of Baldini et al., 2010 and Smith et al., 2016. (For interpretation of the references to colour in this figure legend, the reader is referred to the web version of this article.)

temperature.

Relative humidity outside the cave varies diurnally and seasonally, ranging from 17 to 100%, while cave relative humidity remains at or near 100% year-round. Highest humidities outside of the cave generally occur during the cool and wet winter season, with values falling through the summer. Over the six years of monitoring, three short-lived ventilation events were observed by sudden decreases in relative humidity inside the cave followed by a return to 100% humidity within days (Fig. 7). The origin of these ventilation events is unknown and warrant further investigation but appear correlated with decreases in cave barometric pressure.

Barometric pressures outside the cave (September 2018–August 2019) range from 949 to 985 mb with an average value of 970 mb (Fig. 9). In comparison, cave barometric pressures exhibit a higher range, with values reaching from 932 to 995 mb, with a six-year average value of 972 mb, nearly identical to outside barometric pressure average (Fig. 7). The range of pressure inside the cave during the limited time interval of the outside series produces a nearly identical range of values.

5. Discussion

5.1. Establishing the potential link between atmospheric variability, precipitation patterns, vegetation density, and climate proxies in Portugal

The behavior of the NAO system and the AH are inextricably linked as both the AH and the Icelandic Low represent the two nodes/action centers that form part of the NAO. A robust correlation exists between the Hurrell PC-based NAO index and SLP in the AH region (Ponte Delgado) (1929–2005; $r^2 = 0.46$; $p < 0.05$). The PC-based NAO index accounts for the non-stationarity of the AH, which is not considered with station-based NAO indices. However calculated, all NAO indices are highly correlated with each other (Trigo et al., 2005). As previously discussed, this relationship extends to Portuguese rainfall. During higher pressure conditions for the AH, rain-bearing weather systems are steered to the north of the Iberian Peninsula and Lisbon and other parts of Portugal remain drier than average (Goodess and Jones, 2002; Hurrell, 1995; Osborn et al., 1999; Qian et al., 2000; Trigo et al., 2002).The correlation between Ponte Delgado SLP and Lisbon precipitation for 1874–2005 is $r^2 = 0.32$ ($p < 0.05$) and the correlation between the Hurrell PC-based NAO index and Lisbon precipitation for 1929–2013 is $r^2 = 0.17$ ($p < 0.05$).

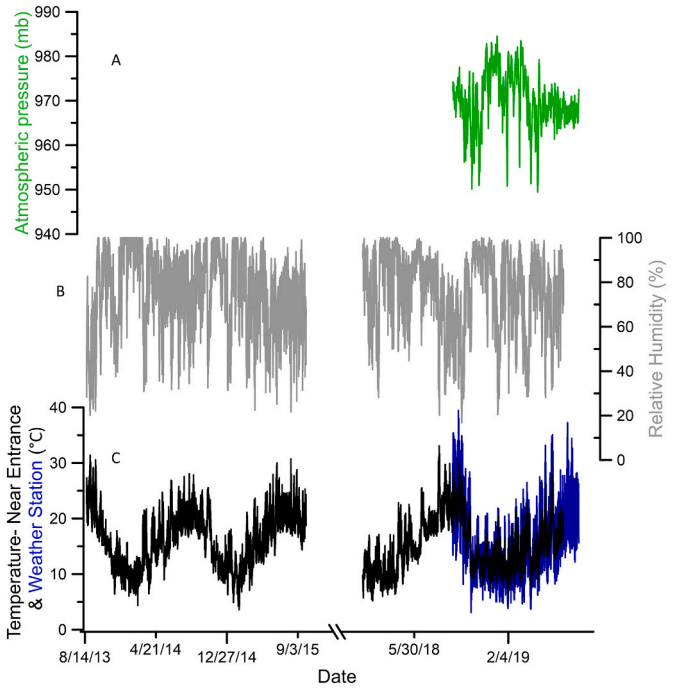

Fig. 9. Environmental monitoring external to BG. A. Barometric pressure outside of BG (green); B. Relative humidity outside of BG (gray); and C. Temperature from two locations outside of BG cave – near the entrance (black) and at the weather station (blue). (For interpretation of the references to colour in this figure legend, the reader is referred to the web version of this article.)

The amount of precipitation influences both the oxygen isotopes of the precipitation as well as the amount of vegetation, as measured here by June–August NDVI, which impacts carbon isotopes. Higher rainfall totals correspond with lower rainwater oxygen isotope ratios at BG (the "amount effect", see following discussion). The amount of precipitation impacts carbon isotopes by increasing vegetation density which causes carbon isotopes of the cave system to more strongly reflect vegetation isotopes rather than rock isotopes.

Particularly in semi-arid climates, such as Portugal, precipitation changes can markedly impact vegetation density and productivity (Cosford et al., 2009). Based on the NDVI map (Fig. 5), there is clear spatial variability in the sensitivity to differences in precipitation across Iberia. Areas in southeast Iberia and north-central Iberia show little difference between the wettest and driest years while western Iberia seems to be more sensitive to these changes in precipitation. Other authors (Gouveia et al., 2008; Vicente-Serrano and Heredia-Laclaustra, 2004) have found significant relationships between NAO and NDVI and it appears that these relationships continue to be robust with the present dataset. Higher NAO indices are associated with decreased precipitation in this region which leads to decreased NDVI. The negative correlation with NDVI and NAO is true for much of Iberia, particularly western Iberia. Western Iberia appears to be an ideal location to study past precipitation dynamics and NAO behavior due to its sensitivity to precipitation-driven vegetation changes.

5.2. Relationship between $\delta^{18}O$ of precipitation, precipitation amount, and mean annual temperature

The current analysis of rainfall isotopes from mainland Portugal and Mira de Aire allows for an investigation of principal impacts on the isotopes of rainfall at BG. Modern precipitation data (GNIP) for ten sites in Portugal help determine general trends in the isotopes of precipitation. There is variability between sites with regards to latitude, altitude, annual average temperature and annual precipitation. Some records from these GNIP sites are incomplete – i.e. missing values for $\delta^{18}O$, $\delta^{2}H$, temperature, and/or precipitation – and some sites have short observation periods (four years or less of data). Considering the limitations of these data, it is still possible to make general observations about oxygen isotope relationships. In general, in Portugal, lower oxygen isotope values of precipitation are associated with higher altitude locations, higher latitude locations, colder locations, and locations which receive more precipitation (Fig. 4). Conversely, higher oxygen isotope values of precipitation are associated with lower altitude locations, lower latitude locations, warmer locations, and locations which receive less precipitation (Fig. 4).

The general observations of controls on Portugal precipitation $\delta^{18}O$ are complemented by an analysis of seasonality of the precipitation $\delta^{18}O$ values. Fig. S3 shows the monthly amount weighted average $\delta^{18}O$ value for each of the ten mainland Portugal GNIP sites as well as the average of value from these ten locations.

A global meta-analysis of 163 drip sites from 39 caves on five continents argued that MAT is ultimately the dominant factor influencing the $\delta^{18}O$ values of dripwater and, thus, of stalagmites (Baker et al., 2019). In areas of the world with a MAT between 10 and 16 °C, such as BG, dripwater represents the recharge-weighted $\delta^{18}O$ value (Baker et al., 2019). At BG, recharge is dominated by Atlantic-sourced winter precipitation (discussion below). The four Portuguese sites with MAT 10–16 °C show average slopes of $\delta^{18}O$-precipitation amount of −2.5‰/100 mm/month and $\delta^{18}O$-temperature of +0.17‰/°C (Fig. S4; Table 1).

For locations with a MAT >16 °C, Baker et al. (2019) proposed that dripwater $\delta^{18}O$ values are likely a compound signal that reflects selective recharge and evaporative fractionation. The four Portuguese sites with MAT >16 °C show average slopes of $\delta^{18}O$-precipitation amount of −2.5‰/100 mm/month and $\delta^{18}O$-temperature of +0.09‰/°C (Fig. S4; Table 1). Finally, for sites with MAT <10 °C, Baker et al. (2019) suggest that the oxygen isotope composition of dripwater is most directly related to the isotopic composition of local rainfall. There is only one such GNIP location in mainland Portugal (Penhas Douradas), and for this site, the $\delta^{18}O$-precipitation amount and $\delta^{18}O$-temperature impacts are −1.0‰/100 mm/month and + 0.12‰/°C, respectively (Fig. S4; Table 1).

These ten mainland Portugal GNIP sites allow for characterization of regional precipitation. Using the monthly amount-weighted averages from all ten Portugal GNIP sites, the amount effect averages −1.8‰ per 100 mm/month precipitation and the temperature effect is +0.16‰ per °C, slightly more than the temperature effect on water-calcite isotope fractionation. As proposed by others, $\delta^{18}O$ values of calcite in speleothems are dominated by the "amount effect" in precipitation from the western Mediterranean (Bard et al., 2002; Denniston et al., 2018; Isola et al., 2019) where increased precipitation leads to lower values of $\delta^{18}O$ of the precipitation. Bard et al. (2002) suggested for a site on the western coast of Italy that the amount effect is −2.0‰/ 100 mm precipitation as opposed to the temperature effect at the same location (+0.3‰/ °C). This temperature effect is roughly equal but opposite in sign to the impact of temperature change on water-calcite isotopic fractionation (−0.2‰ per °C, Kim and O'Neil, 1997). Given the length of the GNIP mainland Portugal record, we conclude that on decadal time scales and longer, lower oxygen isotope values in the calcite are associated with more humid conditions and higher values associated with drier conditions (Drysdale et al., 2004; Regattieri et al., 2014; Zanchetta et al., 2007).

These GNIP sites are complemented by our analysis of isotopes in precipitation from Mira de Aire, a site much closer to BG than any of the GNIP sites and at a similar elevation to BG. From the 108 rainfall events collected between September 2018 and November 2019 at Mira de Aire, relationships between $\delta^{18}O$-precipitation amount and $\delta^{18}O$-temperature are $r^2 = 0.18$ ($p < 0.05$) and $r^2 = 0.08$ ($p < 0.05$), respectively (Fig. 10). When binned monthly and adjusted to amount-weighted $\delta^{18}O$ values, the relationships are more highly correlated. The amount effect is particularly prominent and statistically significant ($r^2 = 0.43$, $p < 0.05$) while air temperature effects are also present ($r^2 = 0.30$, $p = 0.08$)

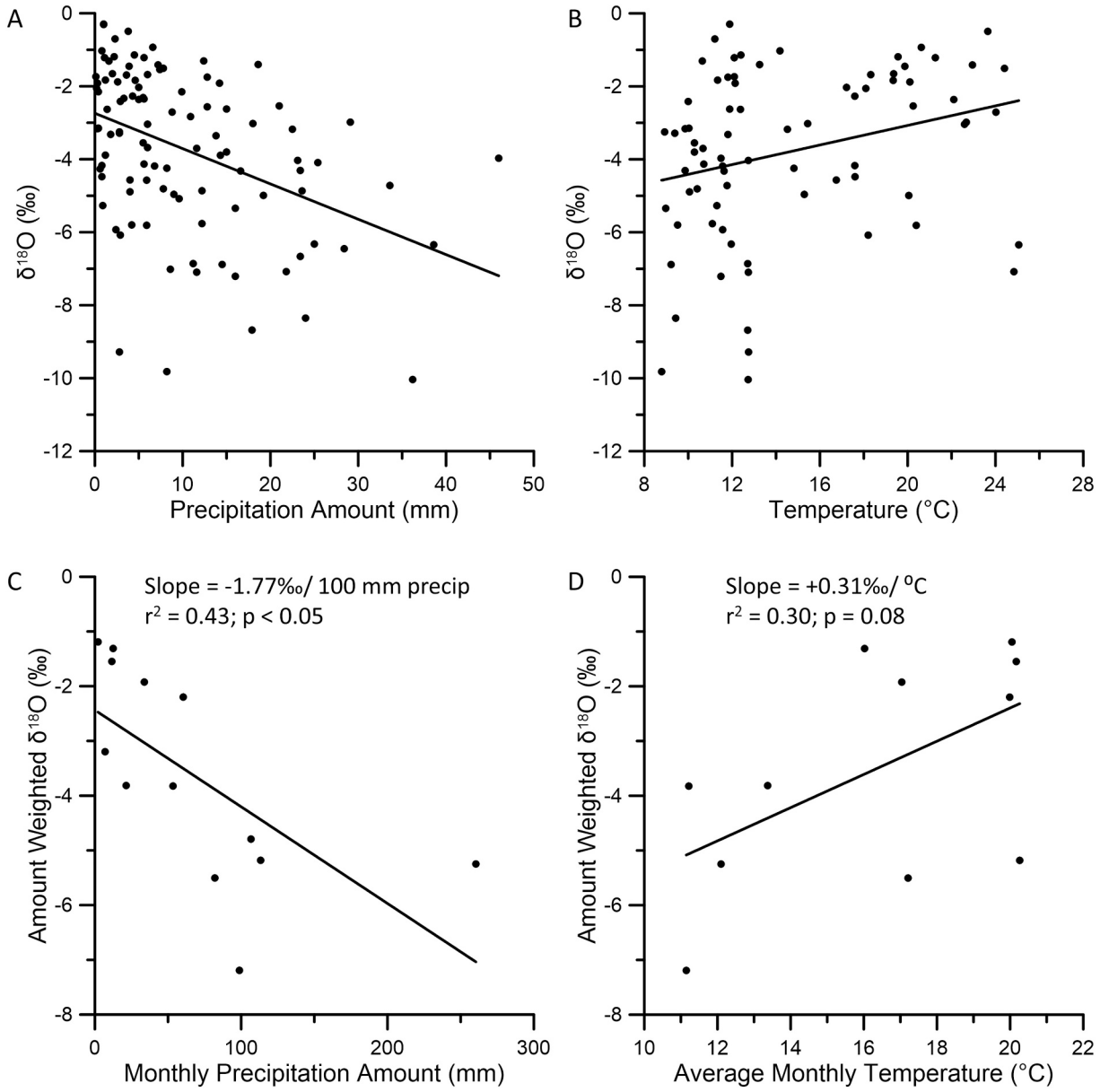

Fig. 10. Mira de Aire Rainfall. A. Relationship between daily rainfall amount and rainfall oxygen isotope measurements; B. Relationship between daily average temperature and rainfall oxygen isotope measurements. C & D are monthly-binned relationships for precipitation amount and temperature, respectively.

however they are less prominent and not significant. The slopes for the $\delta^{18}O$-precipitation amount and $\delta^{18}O$-temperature lines are −1.77‰/100 mm/month and + 0.31‰/°C (Fig. 10) for the monthly-binned values of precipitation from Mira de Aire. Following the logic of Bard et al. (2002) as outlined above, the +0.31‰/°C would be mostly offset by the impact of temperature change on water-calcite isotopic fractionation (−0.2‰/°C, Kim and O'Neil, 1997). The amount effect is also visually apparent when considering the time series of isotopes from Mira de Aire as lower values of oxygen isotopes are associated with higher amounts of precipitation (Fig. S2). In this region, it is likely that the precipitation amount is impacting the $\delta^{18}O$ values of precipitation with temperature effects less impactful on precipitation isotope values (Denniston et al., 2018) and the recharge is dominated by winter Atlantic-sourced precipitation. The drip water isotope values from BG are similar to the winter precipitation isotopes from Mira de Aire (Fig. 6C) confirming the relationship of recharge and winter precipitation.

Finally, comparison of drip water and rainwater allow for some constraints on the degree of homogenization of percolating fluids in the bedrock (Cobb et al., 2007; Mattey et al., 2008; Perrin and Jeannin, 2003). Although several dripwater measurements were made on time-integrated samples, the oxygen (and hydrogen) isotopes for precipitation and drip water are similar but the variability in the precipitation isotopes is smaller for the drip water isotopes (Fig. 6A). The average precipitation isotopes from Mira de Aire fall directly within the range of dripwater isotopes from BG (Fig. 6) indicating that studying BG dripwater (and thus stalagmites) is a robust way of assessing past precipitation and atmospheric dynamics in this region.

5.3. Source impacts on oxygen isotopes of dripwater

Dripwater flowing through the overlying rock and into the cave originated as precipitation falling above the cave. The isotopes of the precipitation at a particular location are principally impacted by three factors: i) the amount of rain falling in the region, and ii) the temperature at which the rain falls; and iii) the source region of the moisture

(Lachniet, 2009). Factors (i) and (ii) were discussed above. According to Lachniet (2009) and others, the source effect is the observation that air masses derived from different moisture sources have distinct $\delta^{18}O$ values (Clark and Fritz, 1997; Cole et al., 1999; Friedman et al., 2002; Rozanski et al., 1993) as the $\delta^{18}O$ values of ocean water vary globally (LeGrande and Schmidt, 2006). The potential and proximal sources of air masses over western Portugal include the Atlantic Ocean and the Mediterranean Sea with oxygen isotope values in the Atlantic-sourced precipitation being several per mil lower than that of the Mediterranean (LeGrande and Schmidt, 2006). Precipitation $\delta^{18}O$ values are sensitive to areas of high evaporation, such as the Mediterranean Sea, thus moisture originating over the Mediterranean would be expected to have an isotopic signal that differs from moisture that originates over the Atlantic Ocean, a less evaporative region (Bowen and Wilkinson, 2002). Such differences in moisture sources have the potential to impact oxygen isotopes of the precipitation falling over BG, if precipitation amounts associated with each moisture source are sufficient to add to recharge.

Larger precipitation events at Mira de Aire have an Atlantic signature and the small number of rain events (5 of 108 events) that do not strongly suggest an Atlantic signature are characterized by little precipitation (all five events are <20 mm and four of the five <6 mm; Fig. 8). Conversely, all of the events >30 mm originated from the northwest of BG and the largest twelve events are all Atlantic-sourced. This suggests that precipitation contributing to recharge at BG is Atlantic-sourced. This result is important for future hydroclimate studies because if the dominant source region of precipitation is consistent over the observation period, then variability in the isotope record is less likely to reflect varying source regions and more likely to reflect changes in precipitation amount.

Additionally, an analysis of the source trajectories of three wettest years and three driest years since 1982 using Lisbon precipitation data yields even more robust conclusions. Fig. 8D shows the air mass trajectories for the three lowest precipitation winters compared to precipitation amount and Fig. 8E the air mass trajectories for the three highest precipitation winters. The driest years have overall less precipitation, fewer precipitation events, fewer large precipitation events (>30 mm/day), and a more variable moisture source. The wettest years have overall more precipitation, more precipitation events, a greater number of large precipitation events (>30 mm/day), and a dominant Atlantic moisture source. As Lisbon is only ~100 km from BG, these conclusions can be broadly applied to the current study site.

5.4. Carbon isotopes in the BG cave system

As discussed above, the carbon in speleothem calcite is derived from three (not necessarily equally contributing) main sources: i) soil respiration-produced CO_2 (−12 to −27‰ depending on vegetation type; Cerling, 1984; Deines, 1980; O'Leary, 1988; VonFischer et al., 2008) ii) atmospheric CO_2 (−6.4‰ prior to major industrialization and ~ −9‰ currently; Graven et al., 2017) and iii) inorganic carbon from the carbonate rocks (average 0‰ but can range from +6 to −3‰) (Cacchio et al., 2004; Cruz et al., 2006; Johnson et al., 2006; Pacton et al., 2013). Changes in the relative contributions from these three sources can cause changes in speleothem $\delta^{13}C$ values. Shifts in the type of vegetation overlying the cave (unlikely during the Holocene; d'Errico and Sánchez Goñi, 2003; Desprat et al., 2006; Margari et al., 2014; Sánchez Goñi et al., 2008, 2013; Tzedakis et al., 2004), changes in degassing with variable drip rates (Mühlinghaus et al., 2007), shifts between open and closed system behavior (Fohlmeister et al., 2011; Hendy, 1971), and/or variable degrees of dissolution of host rock also impact carbon isotope values.

The soil above BG has average $\delta^{13}C$ values of −28.9 ± 0.3‰, the vegetation above the cave has an average value of $\delta^{13}C$ of −26.8 ± 0.2‰, and the rock has an average value of +3.1 ± 1.0‰ (Denniston et al., 2018). These carbon isotope values indicate that the type of vegetation above BG cave is dominantly C_3 (nominal vales of about −27‰; Cerling, 1984; Deines, 1980; Kohn, 2010; O'Leary, 1988; VonFischer et al., 2008). The past atmospheric $\delta^{13}C$ value can be approximated as ~ − 6.4‰ (Francey et al., 1999). The relative contributions of these carbon sources influence the $\delta^{13}C$ values of the stalagmite in the

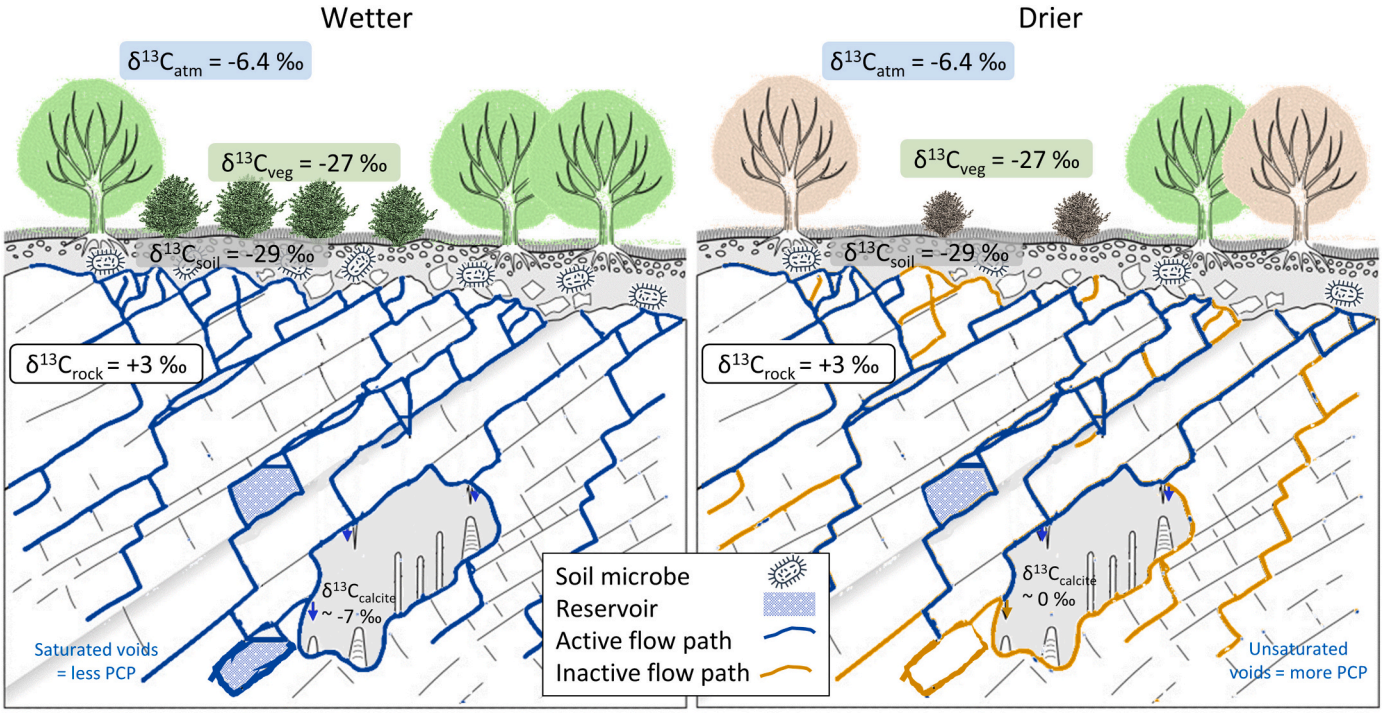

Fig. 11. Adapted from Bradley et al. (2010). Schematic of vegetation density carbon isotopes at BG cave during A. Wetter conditions and B. Drier conditions. Atmospheric CO_2 carbon isotope values are pre-industrial values (current values ~ − 9‰; Francey et al., 1999; Graven et al., 2017). Cave $\delta^{13}C_{calcite}$ values reflect representative values from BG Cave (Thatcher et al., 2020).

caves differently during wetter and drier conditions (Fig. 11). The isotopic values of the three components (soil/vegetation, atmosphere, rock) are not expected to change under these two climatic conditions, however, the $\delta^{13}C$ of dissolved inorganic carbon of the percolating water is expected to vary due to increased/decreased influences of these three components. During wetter conditions, the density of vegetation increases (increased NDVI, Fig. 5), minimizing contributions from atmospheric CO_2 as percolating waters move faster through the karst with less PCP (Fig. 11A), decreasing dripwater carbon isotope values. During drier conditions, vegetation density decreases as indicated by the vegetation index values and PCP also increases (Fig. 5; Fig. 11B; Baldini et al., 2005; Fohlmeister et al., 2020; Genty et al., 2003) resulting in higher carbon isotope ratios.

Considering post precipitation processes and kinetic isotope effects are important when utilizing stalagmites for paleoclimate studies. At BG, evaporation at the land surface and/or kinetic isotope effects may impact stalagmite isotope values. If these processes are occurring, they would shift isotope values in the same direction as would be expected for climate-induced carbon isotope shifts (e.g. evaporation would cause an additional increase in $\delta^{13}C$ values shifting values in the same direction as other dry condition processes). Studies utilizing stalagmites from BG cave have relied on replication to evaluate the impacts of equilibrium vs. secondary effects, including kinetic and evaporation, on isotopic variability (Denniston et al., 1999; Mickler et al., 2004; Thatcher et al., 2020).

5.5. Suitability of BG Cave for paleoclimate studies

Patterns of cave air temperatures closely follow the patterns of outside cave temperatures (Figs. 7 and 9). As described by Wigley and Brown (1976), summer temperatures in the cave are buffered by the heating of the bedrock, resulting in a steady temperature rise. In winter, external air temperature falls and colder, external air can flow into the cave. In BG, this pattern of slow, steady temperature rises in the summer and more sudden temperature decreases in the fall are apparent from the approximately six years of cave monitoring data.

An ideal cave environment for stalagmites that provide robust paleoclimate reconstructions includes consistent temperature and relative humidity as variability in these parameters would complicate paleoclimatic interpretations. The range of variability in temperature inside BG is 1.04 °C throughout the approximately six years of monitoring making BG suitable for paleoclimate studies. Relative humidity is at or near 100% throughout the monitoring period. However, three "ventilation events" have been recorded and are evident as times where the relative humidity briefly falls below 100% inside of the cave. Since these events are short-lived and infrequent, they would not be expected to noticeably impact calcite formation. Dripwater temperatures (Fig. 7) vary on a similar timescale to the cave air temperature although the range is slightly smaller. For two of the three studied winters, the temperature of the dripwater did not cool as much as the cave air temperature.

Drip sites displayed constant dripping during the studied years and were influenced by seasonal differences in precipitation (Fig. 7). Individual drip sites show distinct drip rates but similar seasonal patterns. The drier time of the year has lower drip rates with a rapid return to higher drip rates after fall rains begin (within 1–2 weeks; Fig. 7). This implies that water moves into the cave chamber within 1–2 weeks as the start of the wetter season saturates the system. This somewhat delayed response gives clues to the storage and mixing of water in voids above the cave that likely occurs before entering the cave. Without a tracer study for this cave system, however, we cannot fully understand the complex flow patterns that likely exist including the presence or absence of piston flow.

6. Conclusion

Changes in atmospheric dynamics, namely the behavior of the AH and the associated NAO, drive shifts in vegetation across Iberia. Changes to vegetation density above BG have the potential to alter carbon isotopes in the dripwater and this speleothem carbonate thereby allowing for paleoclimate interpretation of carbon isotopes as a paleoprecipitation proxy.

In general, precipitation amount is the dominant factor in $\delta^{18}O$ values of rain falling across western Portugal, with temperature playing a secondary role. However, variability exists between Portugal locations as to which is the dominant factor controlling $\delta^{18}O$ values of dripwater (selective recharge and evaporative fractionation, recharge-weighted $\delta^{18}O$ value, or local rainfall) and expected impacts vary at different locations based on regional MAT.

At BG, moisture source effects are also critical. Approximately 89% of rainfall over the fifteen months of monitoring at Mira de Aire was derived from the North Atlantic Ocean. These Atlantic-sourced precipitation events are larger and thus likely the dominant influence on recharge in the area. As the MAT in BG is 14.3 °C, changes in $\delta^{18}O$ values of the dripwater are strongly related to $\delta^{18}O$ values of recharge, predominantly Atlantic-sourced winter precipitation, as predicted by the work of Baker et al. (2019).

The six year cave monitoring program at BG has strengthened our understanding of the karst environment in which these speleothems have grown and shows that the cave maintains stable temperature and relative humidity, and that drips within the cave occur year-round but respond to seasonal changes in rainfall. Based on the analyses presented here, we suggest that speleothems sampled from BG would primarily reflect the past hydroclimate of Portugal. Given its ideal location within the center of action of the Azores High (and NAO), this cave is well-suited for studying past atmospheric dynamics over recent millennia.

A main goal of this paper is to evaluate the processes by which changes in atmospheric behavior can be recorded in stalagmites from western Portugal. A simplified description follows. Changes in the NAO index are indicative of changes in AH SLP. When the NAO is positive, SLP is higher in the AH and Iberian Peninsula, and thus, regional precipitation amounts are reduced in this region due to changes in the trajectory of rain-bearing weather systems. Drier conditions over the Iberian Peninsula are associated with higher values of $\delta^{18}O$ of the precipitation which are in turn transmitted to cave dripwater and then to BG stalagmites. Similarly, reductions in annual precipitation decrease vegetation density in Iberia, enhancing the contribution of atmospheric and bedrock carbon to cave dripwater (and diminishing that from vegetation and soil carbon), and thus elevating carbon isotope ratios.

Declaration of Competing Interest

The authors declare that they have no known competing financial interests or personal relationships that could have appeared to influence the work reported in this paper.

Acknowledgements

Use of the following observational-based data sets is gratefully acknowledged: GPCC precipitation data provided by the NOAA/OAR/ESRL PSL, Boulder, Colorado, USA, from their website at https://psl.noaa.gov/; NOAA Climate Data Record of AVHRR Normalized Difference Vegetation Index (NDVI), Version 5, accessed through the NCEI geoportal. We thank Ivan Lima for help with obtaining the NDVI data. This work was supported, in part, by the US National Science Foundation (grants: #1804528 to ADW; #1804635 to RD; #1804132 to CCU; #1805163 to DPG). Special thanks to Jace Bricker, Gabi Hiatt, Stephen Rasin, Hannah Thatcher, and Jayna Wanamaker for their assistance with field work. We would like to thank Jens Fohlmeister and two anonymous reviewers for their helpful comments which substantially improved this

manuscript.

Appendix A. Supplementary data

Supplementary data to this article can be found online at https://doi.org/10.1016/j.chemgeo.2020.119949.

References

Ait Brahim, Y.A., Wassenburg, J.A., Cruz, F.W., Sifeddine, A., Scholz, D., Bouchaou, L., Dassié, E.P., Jochum, K.P., Edwards, R.L., Cheng, H., 2018. Multi-decadal to centennial hydroclimate variability and linkage to solar forcing in the Western Mediterranean during the last 1000 years. Sci. Rep. 8, 17446.

Allan, M., Fagel, N., Van Rampelbergh, M., Baldini, J., Riotte, J., Cheng, H., Edwards, L., Gillikin, D.P., Quinif, Y., Verheyden, S., 2015. Lead concentrations and isotope ratios in speleothems as proxies for atmospheric metal pollution since the Industrial Revolution. Chem. Geol. 401, 140–150. https://doi.org/10.1016/j.chemgeo.2015.02.035.

Andreo, B., Liñán, C., Carrasco, F., Jimenez de Cisneros, C., Caballero, F., Mudry, J., 2004. Influence of rainfall quantity on the isotopic composition (^{18}O and ^{2}H) of water in mountainous areas. Application for groundwater research in the Yunquera-Nieves karst aquifers (S. Spain). Appl. Geochem. 19, 561–574.

Araguas-Araguas, L.J., Diaz Teijeiro, M.F., 2005. Isotope composition of precipitation and water vapour in the Iberian peninsula (IAEA-TECDOC–1453). International Atomic Energy Agency (IAEA).

Asmerom, Y., Baldini, J.U.L., Prufer, K.M., Polyak, V.J., Ridley, H.E., Aquino, V.V., Baldini, L.M., Breitenbach, S.F.M., Macpherson, C.G., Kennett, D.J., 2020. Intertropical convergence zone variability in the Neotropics during the Common Era. Sci. Adv. 6 https://doi.org/10.1126/sciadv.aax3644.

Baker, A., Ito, E., Smart, P.L., McEwan, R.F., 1997. Elevated and variable values of d13C in speleothems in a British cave system. Chem. Geol. 136, 263–270.

Baker, A., Hartman, A., Duan, W., Hankin, S., Comas-Bru, L., Cuthbert, M.O., Treble, P. C., Banner, J., Genty, D., Baldini, L.M., 2019. Global analysis reveals climatic controls on the oxygen isotope composite of cave drip water. Nat. Commun. https://doi.org/10.1038/s41467-019-11027-w.

Baldini, J.U.L., McDermott, F., Baker, A., Baldini, L.M., Mattey, D.P., Railsback, L.B., 2005. Biomass effects on stalagmite growth and isotope ratios: A 20th century analogue from Wiltshire, England. Earth Planet. Sci. Lett. 240, 486–494.

Baldini, J.U.L., Baldini, L.M., McDermott, F., Clipson, N., 2006. Carbon dioxide sources, sinks, and spatial variability in shallow temperate zone caves: evidence from Ballynamintra Cave, Ireland. J. Cave Karst Stud. 68, 4–11.

Baldini, L.N., McDermott, F., Baldini, J.U.L., Fischer, M.J., Möllhoff, M., 2010. An investigation of the controls on Irish precipitation $\delta^{18}O$ values on monthly and event timescales. Clim. Dyn. 35, 977–993.

Bard, E., Delaygue, G., Rostek, F., Antonioli, F., Silenzi, S., Schrag, D.P., 2002. Hydrological conditions over the western Mediterranean basin during the deposition of the cold Sapropel 6 (ca. 175 kyr BP). Earth and Planetary Science letters 202, 481–494.

Bowen, G.J., Wilkinson, B., 2002. Spatial distribution of δ18O in meteoric precipitation. Geology 30, 315–318.

Bradley, C., Baker, A., Jex, C.N., Leng, M.J., 2010. Hydrological uncertainties in the modelling of cave drip-water $\delta^{18}O$ and the implications for stalagmite palaeoclimate reconstructions. Quat. Sci. Rev. 29, 2201–2214.

Cacchio, P., Contento, R., Ercole, C., Cappuccio, G., Oreite-Martinex, M., Lepidi, A., 2004. Involvement of Microorganisms in the Formation of Carbonate Speleothems in the Cervo Cave (L'Aquila-Italy). Geomicrobiol J. 21, 497–509.

Carreira, P.M.M., Araujo, M.F., Nunes, D., 2005. Isotopic composition of rain and water vapour samples from Lisbon region: Characterization of monthly and daily events. In: Isotopic Composition of precipitation in the Mediterranean Basin in Relation to Air Circulation Patterns And Climate. IAEA. October 2005.

Celle, 2000. Caractérisation Des Précipitations Sur Le Pourtour De La Méditerranée Occidentale –Approche Isotopique Et Chimique. PhD Thesis. Université d'Avignon.

Cerling, T., 1984. The stable isotopic composition of modern soil carbonate and its relationship to climate. Earth Planet. Sci. Lett. 71, 229–240.

Cheng, H., Edwards, R.L., Sinha, A., Spötl, C.L., Yi, L., Chen, S., Kelly, M., Kathayat, G., Wang, X., Li, X., Kong, X., Wang, Y., Ning, Y., Zhang, H., 2016. The Asian monsoon over the past 640,000 years and ice age terminations. Nature 534, 640–646. https://doi.org/10.1038/nature18591pmid:27357793.

Clark, I., Fritz, P., 1997. Environmental Isotopes in Hydrogeology. Lewis Publishers, Boca Raton & New York.

Cobb, K.M., Clark, B., Partin, J.W., Adkins, J.F., 2007. Regional-scale climate influences on temporal variations in rainwater and cave dripwater oxygen isotopes in northern Borneo. Earth Planet. Sci. Lett. 263, 207–220.

Cole, J.E., Rind, D., Webb, R.S., Jouzel, J., Healy, R., 1999. Climate controls on interannual variability of precipitation $\delta^{18}O$: simulated influence of temperature, precipitation amount, and vapor source region. J. Geophys. 104, 14,223–14,235.

Collister, C., Mattey, D., 2008. Controls on water drop volume at speleothem drip sites: An experimental study. J. Hydrol. 358, 259–267.

Cosford, J., Qing, H., Mattey, D., Eglington, B., Zhang, M., 2009. Climate and local effects on stalagmite $\delta^{13}C$ values and Lianhua Cave, China. Palaeogeogr. Palaeoclimatol. Palaeoecol. 280, 235–244.

Craig, H., 1961. Isotopic Variations in Meteoric Waters. Science 133, 1702–1703.

Cruz, F.W., Burns, S.J., Karmann, I., Sharp, W.D., Vuille, M., Ferrari, J.A., 2006. A stalagmite record of changes in atmospheric circulation and soil processes in the Brazilian subtropics during the late Pleistocene. Quat. Sci. Rev. 25, 2749–2761.

Dansgaard, W., 1964. Stable isotopes in precipitation. Tellus 4, 436–468.

Davis, R.E., Hayden, B.P., Gay, D.A., Phillips, W.L., Jones, G.V., 1997. The North Atlantic Subtropica Anticyclone. J. Clim. 10, 728–744.

Deines, P., 1980. The isotopic composition of reduced organic carbon. In: Fritz, Peter, Fontes, Jean-Charles (Eds.), 1980. Handbook of Environmental Isotope Geochemistry, 1. Elsevier, New York, pp. 329–406.

Denniston, R.F., González, L.A., Baker, R.G., Asmerom, Y., Reagan, M.K., Edwards, R.L., Alexander, E.C., 1999. Speleothem evidence for Holocene fluctuations of the prairie-forest ecotone, north-Central USA. The Holocene 9, 671–676.

Denniston, R.F., Houts, A.N., Asmerom, Y., Wanamaker, A.D., Haws, J.A., Polyak, V.J., Thatcher, D.L., Altan-Ochir, S., Borowske, A.C., Breitenbach, S.F.M., Ummenhofer, C.C., Regala, F.T., Benedetti, M.M., Bicho, N.F., 2018. A stalagmite test of North Atlantic SST and Iberian hydroclimate linkages over the last two glacial cycles. Clim. Past 14, 1893–1913.

d'Errico, F., Sánchez Goñi, M.F., 2003. Neandertal extinction and the millennial scale climatic variability of OIS 3. Quat. Sci. Rev. 22, 769–788.

Desprat, S., Sánchez Goñi, M.F., T, J.-L., Duprat, J., Malaizé, B., Peypouquet, J.-P., 2006. Climatic variability of Marine Isotope Stage 7: direct land-sea-ice correlation from a multiproxy analysis of a north-western Iberian margin deep-sea core. Quat. Sci. Rev. 25, 1010–1026.

Draxler, R.R., Hess, G.D., 1998. An overview of the HYSPLIT 4 modelling system for trajectories, dispersion, and deposition. Aust. Meteorol. Mag. 47, 295–308.

Draxler, R.R., Rolph, G.D., 2003. HYSPLIT (HYbrid Single-Particle Lagrangian Integrated Trajectory) Model access via NOAA ARL READY Website, NOAA Air Resour. Lab. Silver Spring, Md available online at. http://www.arl.noaa.gov/ready/hysplit4.html .

Drysdale, R.N., Zanchetta, G., Hellstrom, J.C., Zhao, J., Fallick, A.E., Isola, I., Bruschi, G., 2004. Palaeoclimatic implications of the growth history and stable isotope ($\delta^{18}O$ and $\delta^{13}C$) geochemistry of a middle to late Pleistocene stalagmite from Central-Western Italy. Earth Planet. Sci. Lett. 227, 215–229.

Dulinski, M., Rozanski, K., 1990. Formation of 13C/12C isotope ratios in speleothems: a semi-dynamic model. Radiocarbon 32, 7–16.

Fairchild, I., Baker, A., 2012. Speleothem Science. Wiley-Blackwell, West Sussex, UK.

Fairchild, I.J., Treble, P.C., 2009. Trace elements in speleothems as recorders of environmental change. Quat. Sci. Rev. 28, 449–468.

Fohlmeister, J., Scholz, D., Kromer, B., Mangini, A., 2011. Modelling carbon isotopes of carbonates in cave drip water. Geochim. Cosmochim. Acta 75, 5219–5228.

Fohlmeister, J., Voarintsoa, N.R.G., Lechleitner, F.A., Boyd, M., Brandtstätter, S., Jacobson, M.J., Oster, J., 2020. Main controls on the stable carbon isotope composition of speleothems. Geochim. Cosmochim. Acta 279, 67–87. https://doi.org/10.1016/j.gca.2020.03.042.

Francey, R.J., Allison, C.E., Etheridge, D.M., Trudinger, C.M., Enting, I.G., Leuenberger, M., Langenfelds, R.L., Michel, E., Steele, L.P., 1999. A 1000-year high precision record of $\delta^{13}C$ in atmospheric CO_2. Tellus 51B, 170–193.

Friedman, I., Harris, J.M., Smith, G.I., Johnson, C.A., 2002. Stable isotope composition of waters in the Great Basin, United States 1. Air-mass trajectories. J. Geophys. Res. 107 https://doi.org/10.1029/2001JD000565.

Genty, D., Blamart, D., Ouahdi, R., Gilmour, M., Baker, A., Jouzel, J., Van-Exter, S., 2003. Precise dating of Dansgaard-Oeschger climate oscillations in western Europe from stalagmite data. Nature 421, 833–837.

Genty, D., Blamart, D., Ghaleb, B., Plagnes, V., Causse, C., Bakalowicz, M., Zouari, K., Chkir, N., Hellstrom, J., Wainer, K., Bourges, F., 2006. Timing and dynamics of the last deglaciation from European and North African delta C-13 stalagmite profiles - comparison with Chinese and South Hemisphere stalagmites. Quat. Sci. Rev. 25, 2118–2142.

Goodess, C.M., Jones, P.D., 2002. Links between circulation and changes in the characteristics of Iberian rainfall. Int. J. Climatol. 22, 1593–1615.

Gouveia, C., Trigo, R.M., 2011. The Impacts of the NAO on the Vegetation activity in Iberia. In: Vicente-Serrano, S., Trigo, R. (Eds.), Hydrological, Socioeconomic and Ecological Impacts of the North Atlantic Oscillation in the Mediterranean Region. Advances in Global Change Research, vol 46. Springer, Dordrecht.

Gouveia, C., Trigo, R.M., DaCamara, C.D., Libonati, R., Pereira, J.M.C., 2008. The North Atlantic Oscillation and European vegetation dynamics. Int. J. Climatol. 28, 1835–1847.

Graven, H., Allison, C.E., Etheridge, D.M., Hammer, S., Keeling, R.F., Lenin, I., Meijer, H. A.J., Rubino, M., Tans, P.P., Trudinger, C.M., Vaughn, B.H., White, J.W.C., 2017. Compiled records of carbon isotopes in atmospheric CO2 for historical simulations in CMIP6. Geosci. Model Dev. 10, 4405–4417.

Hendy, C., 1971. The isotopic geochemistry of speleothems – I. the calculation of the effects of different modes of formation on the isotopic composition of speleothems and their applicability as palaeoclimatic indicators. Geochim. Cosmochim. Acta 35, 801–824.

Hou, J.Z., Tan, M., Cheng, H., Liu, T.S., 2003. Stable isotope records of plant cover change and monsoon variation in the past 2200 years: evidence from laminated stalagmites in Beijing, China. Boreas 32, 304–313.

Hurrell, J.W., 1995. Decadal Trends in the North Atlantic Oscillation: Regional Temperatures and Precipitation. Science 269, 676–679.

Hurrell, J.W., Deser, C., 2009. North Atlantic climate variability: the role of the North Atlantic Oscillation. J. Mar. Syst. 78, 28–41.

IAEA/WMO, 2020. Global Network of Isotopes in Precipitation, The GNIP Database available at. http://www.iaea.org/water. last access: 2020.

Isola, I., Zanchetta, G., Drysdale, R.N., Regattieri, E., Bini, M., Bajo, P., Hellstrom, J.C., Baneschi, I., Lionello, P., Woodhead, J., Greig, A., 2019. The 4.2 ka BP event in the

Central Mediterrean: New data from a Corchia speleothem (Apuan Alps, Central Italy). Clim. Past 15, 135–151.
Jambrina-Enríquez, M., Rico, M., Moreno, A., Leira, M., Bernárdez, P., Prego, R., Recio, C., Valero-Garcés, B.L., 2014. Timing of deglaciation and postglacial environmental dynamics in NW Iberia: the Sanabria Lake record. Quat. Sci. Rev. 94, 136–158.
Johnson, K.R., Hu, C., Belshaw, N.S., Henderson, G.M., 2006. Seasonal trace-element and stable-isotope variations in a Chinese speleothem: the potential for high-resolution paleomonsoon reconstruction. Earth Planet. Sci. Lett. 244, 394–407.
Karnieli, A., Agam, N., Pinker, R.T., et al., 2010. Use of NDVI and land surface temperature for drought assessment: merits and limitations. J. Clim. 23, 618–633.
Kim, S., O'Neil, J.R., 1997. Equilibrium and nonequilibrium oxygen isotope effects in synthetic carbonates. Geochim. Cosmochim. Acta 61, 3461–3475.
Kohn, M.J., 2010. Carbon isotope compositions of terrestrial C3 plants as indicators of (paleo)ecology and (paleo)climate. Proc. Natl. Acad. Sci. 107, 19691–19695.
Kutiel, H., Trigo, R.M., 2014. The rainfall regime in Lisbon in the last 150 years. Theor. Appl. Climatol. 118, 387–403.
Lachniet, M., 2009. Climatic and environmental controls on speleothem oxygen-isotope values. Quat. Sci. Rev. 28, 412–432.
LeGrande, A.N., Schmidt, G.A., 2006. Global gridder data set of the oxygen isotopic composition of seawater. Geophys. Res. Lett. 33 https://doi.org/10.1029/2006GL026011.
Margari, V., Skinner, L.C., Hodell, D.A., Martrat, B., Toucanne, S., Grimalt, J.O., Gibbard, P.L., Lunkka, J.P., Tzedakis, P.C., 2014. Land-ocean changes on orbital and millennial time scales and the penultimate glaciation. Geology 42, 183–186.
Martín-Chivelet, J., Muñoz-Garcia, M.B., Edwards, R.L., Turrero, M.J., Ortega, A.I., 2011. Land surface temperature changes in Northern Iberia since 4000 yr BP, based on $\delta^{13}C$ of speleothems. Glob. Planet. Chang. 77, 1–12.
Mattey, D., Lowry, D., Duffet, J., Fisher, R., Hodge, E., Frisia, S., 2008. A 53 year seasonally resolved oxygen and carbon isotope record from a modern Gibraltar speleothem: reconstructed drip water and relationship to local precipitation. Earth Planet. Sci. Lett. 269, 80–95.
McDermott, F., 2004. Palaeo-climate reconstruction from stable isotope variations in speleothems: a review. Quat. Sci. Rev. 23, 901–918.
Meyer, K.W., Feng, W., Breecker, D.O., Banner, J.L., 2014. Interpretation of speleothem calcite d13C variations: evidence from monitoring soil CO2, drip water, and modern speleothem calcite in Central Texas. Geochim. Cosmochim. Acta 142. https://doi.org/10.1016/j.gca.2014.07.027.
Mickler, P.J., Banner, J.L., Stern, L., Asmerom, Y., Edwards, R.L., Ito, E., 2004. Stable isotope variations in modern tropical speleothems: evaluating equilibrium vs. kinetic isotope effects. Geochim. Cosmochim. Acta 68, 4381–4393.
Mühlinghaus, C., Schola, D., Mangini, A., 2007. Modelling fractionation of stable isotopes in stalagmites. Geochimica et Cosmochimica Act 73, 7275–7289.
National Center for Atmospheric Research Staff (Ed.), 2018. The Climate Data Guide: NDVI: Normalized-difference-vegetation-index: NOAA AVHRR. Last modified 14 Mar. Retrieved from. https://climatedataguide.ucar.edu/climate-data/ndvi-normalized-difference-vegetation-index-noaa-avhrr.
National Center for Atmospheric Research Staff (Ed.), 2019. The Climate Data Guide: Hurrell North Atlantic Oscillation (NAO) Index (PC-based). Last modified 10 Sep. Retrieved from. https://climatedataguide.ucar.edu/climate-data/hurrell-north-atlantic-oscillation-nao-index-pc-based.
O'Leary, M.H., 1988. Carbon Isotopes in Photosynthesis. Bioscience 38, 328–336.
Osborn, T.J., Briffa, K.R., Tett, S.F.B., Jones, P.D., Trigo, R.M., 1999. Evaluation of the North Atlantic Oscillation as simulated by a coupled climate model. Clim. Dyn. 15, 685–702.
Osterlin, C., 2010. Stable Carbon Isotopes in Speleothems from Temperature Areas. Stockholm University.
Pacton, M., Breitenbach, S.F.M., Lechleitner, F.A., Vaks, A., Rollion-Bard, C., Gutareva, O.S., Osintcev, A.V., Vasconcelos, C., 2013. The role of microorganisms in the formation of a stalactite in Botovskaya Cave, Siberia – paleoenvironmental implications. Biogeosciences 10, 6115–6130.
Perrin, J., Jeannin, P.-Y., 2003. Epikarst storage in a karst aquifer: A conceptual model based on isotopic data, Milandre test site, Switzerland. J. Hydrol. 279, 106–124.
Pla, S., Catalan, J., 2005. Chrysophyte cysts from lake sediments reveal the submillennial winter/spring climate variability in the northwestern Mediterranean region throughout the Holocene. Clim. Dyn. 24, 263–278.
Pla-Rabes, S., Catalan, J., 2011. Deciphering chrysophyte responses to climate seasonality. J. Paleolimnol. 46, 139–150.
Qian, B., Corte-Real, J., Ad Xu, H., 2000. Is the North Atlantic Oscillation the most important atmospheric pattern for precipitation in Europe? J. Geophys. Res. 105, 11,901–11, 910.
Regattieri, E., Zanchetta, G., Drysdale, R.N., Isola, I., Hellstrom, J.C., Dallai, L., 2014. Lateglacial to Holocene trace element record (Ba, Mg, Sr) from Corchia Cave (Apuan Alps, Central Italy): paleoenvironmental implications. J. Quat. Sci. 29, 381–392.
Rodrigues, M., Fonseca, A., 2010. Geoheritage assessment based on large-scale geomorphological mapping: contributes from a Portuguese limestone massif example. Geomorphologie: Relief, Processus, Environ. 2, 189–198.
Rozanski, K., Araguás-Araguás, L., Gonfiantini, R., 1993. Isotopic patterns in modern global precipitation. In: Swart, P.K., Lohmann, K.C., McKenzie, J., Savin, S. (Eds.), Climate Change in Continental Isotopic Records, Geophysical Monograph, vol. 78. American Geophysical Union, Washington, D.C., pp. 1–36
Sáez de Cámara, E., Gangoiti, G., Alonso, L., Iza, J., 2015. Daily precipitation in Northern Iberia: Understanding the recent changes after the circulation variability in the North Atlantic sector. JGR-Atmos. 120, 9981–10,005. https://doi.org/10.1002/2015JD023306.
Salomon, W., Mook, W.G., 1986. Isotope geochemistry of carbonates in the weathering zone. In: Fritz, P., Fontes, J.C. (Eds.), Handbook of Environmental Isotopes Geochemistry, vol. 1. Elsevier, Amsterdam, pp. 239–265.
Sánchez Goñi, M.F., Landais, A., Fletcher, W.J., Naughton, F., Desprat, S., Duprat, J., 2008. Contrasting impacts of Dansgaard-Oeschger events over a western European latitudinal transect modulated by orbital parameters. Quat. Sci. Rev. 27, 1136–1151.
Sánchez Goñi, M.F., Bard, E., Landais, A., Rossignol, L., d'Errico, F., 2013. Air-sea temperature decoupling in western Europe during the last interglacial-glacial transition. Nat. Geosci. 6, 837–841.
Sanchez, E., Dominguez, M., Romera, R., Lopex de la Franca, N., Gaertner, M.A., Gallardo, C., Castra, M., 2011. Regional modeling of dry spells over the Iberian Peninsula for present climate and climate change conditions. Climate Change 107, 625–634. https://doi.org/10.1007/s10584-011-0114-9.
Sánchez-López, G., Hernández, A., Pla-Rabes, S., Trigo, R.M., Toro, M., Granados, I., Sáez, A., Masqué, P., Pueyo, J.J., Rubio-Inglés, M.J., Giralt, S., 2016. Climate reconstruction for the last two millennia in Central Iberia: the role of East Atlantic (EA), North Atlantic Oscillation (NAO) and their interplay over the Iberian Peninsula. Quat. Sci. Rev. 149, 135–150.
Schneider, U., Becker, A., Finger, P., Meyer-Christoffer, A., Ziese, M., Rudolf, B., 2014. GPCC's new land surface precipitation climatology based on quality-controlled in situ data and its role in quantifying the global water cycle. Theor. Appl. Climatol. 115, 15–40.
Serreze, M.C., Carse, F., Barry, R.G., Rogers, J.C., 1997. Icelandic Low cyclone activity: Climatological features, linkages with the NAO, and relationships with recent changes in the Northern Hemisphere circulation. J. Clim. 10, 453–464.
Smith, A.C., Wynn, P.M., Barker, P.A., Leng, M.J., Noble, S.R., Stott, A., 2016. Cave monitoring and the potential for palaeoclimate reconstruction from Cueva de Asiul, Cantabria (N. Spain). Int. J. Speleol. 45, 1–9.
Stoll, H.M., Moreno, A., Mendez-Vicente, A., Gonzalez-Lemos, S., Jimenex-Sanchez, M., Dominguez-Cuesta, M.J., Edwards, R.L., Cheng, H., Wang, X., 2013. Paleoclimate and growth rates of speleothems in the northwestern Iberian Peninsula over the last two glacial cycles. Quat. Res. 80, 284–290.
Thatcher, D.L., Wanamaker, A.D., Denniston, R.D., Asmerom, Y., Polyak, V., Fullick, D., Ummenhofer, C.C., Gillikin, D.P., Haws, J., 2020. Hydroclimate Variability from Western Iberia (Portugal) during the Holocene – Insights from a Composite Stalagmite Isotope Record. The Holocene. https://doi.org/10.1177/0959683620908648.
Treble, P., Shelley, J.M.G., Chappell, J., 2003. Comparison of high-resolution sub-annual records of trace elements in a modern (1911-1992) speleothem with instrumental climate data from Southwest Australia. Earth Planet. Sci. Lett. 216, 141–153.
Trigo, R.M., Osborn, T.J., Corte-Real, J.M., 2002. The North Atlantic Oscillation influence on Europe: climate impacts and associated physical mechanisms. Clim. Res. 20, 9–17.
Trigo, R.M., Pozo-Vázquez, D., Osborn, T.J., Castro-Díez, Y., Gámiz-Fortis, S., Esteban-Parra, M.J., 2004. North Atlantic Oscillation Influence on precipitation, river flow and water resources in the Iberian Peninsula. Int. J. Climatol. 24, 925–944.
Trigo, R.M., Zêzere, J.L., Rodrigues, M.L., Trigo, I.F., 2005. The Influence of the North Atlantic Oscillation on Rainfall triggering of Landslides near Lisbon. Nat. Hazards 36, 331–354.
Tucker, C.J., 1979. Red and photographic infrared linear combinations for monitoring vegetation. Remote Sens. Environ. 8, 127–150.
Tzedakis, P.C., Roucoux, K.H., de Abreu, L., Shackleton, N.J., 2004. The duration of forest stages in southern Europe and interglacial climate variability. Science 306, 2231–2235.
Ulbrich, U., Christoph, M., 1999. A shift of the NAO and increasing storm track activity over Europe due to anthropogenic greenhouse gas forcing. Clim. Dyn. 15, 551–559.
van Loon, H., Rogers, J.C., 1978. The Seesaw in Winter Temperatures between Greenland and Northern Europe. Part I: General Description. Mon. Weather Rev. 106, 296–310.
Vicente-Serrano, S.M., Heredia-Laclaustra, A., 2004. NAO influence on NDVI trends in the Iberian peninsula (1982-2000). Int. J. Remote Sens. 25, 2871–2879.
Vicente-Serrano, S.M., et al., 2011. The NAO Impact on Droughts in the Mediterranean Region. In: Vicente-Serrano, S., Trigo, R. (Eds.), Hydrological, Socioeconomic and Ecological Impacts of the North Atlantic Oscillation in the Mediterranean Region. Advances in Global Change Research, vol 46. Springer, Dordrecht.
VonFischer, J.C., Tieszen, L.L., Schimel, D.S., 2008. Climate controls on C3 vs. C4 productivity in north American grasslands from carbon isotope composition of soil organic matter. Glob. Chang. Biol. 14, 1141–1155. https://doi.org/10.1111/j.1365-2486.2008.01552.x.
Wainer, K., Genty, D., Blamart, D., Hoffman, D., Couchoud, I., 2009. A new stage 3 millennial climatic variability records from a SW France speleothem. Palaeogeogr. Palaeoclimatol. Palaeoecol. 271, 130–139.
Wang, Y., Cheng, H., Edwards, R.L., He, Y., Kong, X., An, Z., Wu, J., Kelly, M.J., Dykoski, C.A., Li, X., 2005. The Holocene Asian Monsoon: Links to Solar changes and North Atlantic climate. Science 308, 854–857.
Wigley, T.M.L., Brown, M.C., 1976. The physics of caves. In: Ford, T.D., Cullingford, C.H. D. (Eds.), The Science of Speleology. Academic Press, London, pp. 329–358.
Xoplaki, E., González-Rouco, J.F., Luterbacher, J., Wanner, H., 2004. Wet season Mediterranean precipitation variability: influence of large-scale dynamics and trends. Clim. Dyn. 23, 63–78.
Zanchetta, G., Borghini, A., Fallick, A.E., Bonadonna, F.P., Leone, G., 2007. Late Quaternary palaeohydrology of Lake Pergusa (Sicily, southern Italy) as inferred by stable isotopes of lacustrine carbonates. J. Paleolimnol. 38, 227–239.